Jpn. J. Genet. (1994) **69**, *pp.* 137–182

Experimental bases for the minimum interaction theory. I. Chromosome evolution in ants of the *Myrmecia pilosula* species complex (Hymenoptera: Formicidae: Myrmeciinae)

Hirotami T. IMAI[1], Robert. W. TAYLOR[2] and Rossiter H. CROZIER[3]

[1]*National Institute of Genetics, Mishima, Shizuoka 411, Japan*
[2]*Division of Entomology, CSIRO, Canberra, ACT 2601, Australia*
[3]*Dept. of Genetics and Human Variation, Latrobe University, Bundoora, Victoria 3083, Australia*

(*Received 17 January 1994*)

ABSTRACT

Chromosome evolution in primitive Australian ants of the *Myrmecia pilosula* species complex is investigated in the context of the minimum interaction theory. Under the minimum interaction theory, selection favors rearrangements tending to reduce the occurrence of deleterious chromosomal mutations, and hence chromosome numbers are expected to increase. The complex is chromosomally highly heterogeneous ($2n = 2 - 32$), and comprises at least 5 karyotypically distinct species: *M. croslandi* ($2n = 2 - 4$), *M. imaii* ($2n = 6 - 8$), *M. banksi* ($2n = 9 - 10$), *M. haskinsorum* ($2n = 12 - 24$), and *M. pilosula* ($2n = 18 - 32$). Statistical considerations using the karyograph method and chromosomal alteration network analysis indicate that chromosome evolution of the complex proceeds as a whole towards increase in chromosome number by centric fission and inversions converting chromosomes from acro- to metacentrics (A$\overline{\text{M}}$-inversion). These conclusions are consistent with the predictions of the minimum interaction theory. Both centric fusion and A$\overline{\text{M}}$-inversion serve to eliminate constitutive heterochromatin (visible as C-bands), which appears to increase in a saltatory fashion after centric fission, probably due to telomere instability. Newly observed phenomena which we term "fusion burst" and "fission burst" suggest that rates of chromosome evolution in *M. pilosula* have fluctuated with time.

1. INTRODUCTION

There is a general tendency in many groups of animals for related biological species to have different numbers of chromosomes. Among ants, for example, the numbers are known to range from $2n = 2$ in some individuals of *Myrmecia croslandi* Taylor (Crosland and Crozier, 1986; Imai and Taylor, 1989) to $2n = 94$ in *Nothomyrmecia macrops* Clark (Imai et al., 1990; for further details see Imai et al., 1988a).

Ants are generally accepted as being a monophyletic group, the family Formicidae of the order Hymenoptera (Hölldobler and Wilson, 1990). Thus it is reasonable to assume that their spectacular chromosomal diversity has been derived

from the initial tally of a common ancestral species. This raises several questions relevant to chromosomal evolution. For example, (1) what was the chromosome number of the common ancestor and (2) can a general rule or set of rules be specified to cover the processes of chromosome number alteration in evolution?

Two alternatives may be postulated (1) the fusion hypothesis and (2) the fission hypothesis. In the former evolution proceeds by decrease in chromosome numbers due to centric fusion, while in the latter the reverse occurs through centric fission. Under the fusion hypothesis the ancestor would have had a relatively high chromosome number, but under the fission hypothesis this number would have been relatively low.

The fusion hypothesis was established many years ago by White (1963, 1973). The fission hypothesis was first proposed by Todd (1970, 1975), but has been largely developed and theoretically elaborated by Imai and co-workers (Imai, 1975, 1976,1978; Imai, Crozier and Taylor,1977; Imai and Maruyama, 1978; Imai and Crozier, 1980).

As central propositions, the fusion hypothesis requires the centromere to have a unitary structure, and it precludes *de novo* formation of the telomere. Recent studies in molecular genetics have revealed, however, that the centromere may be compound, due to multiplication of the primary functional unit, and that *de novo* formation of the telomere does occur through the action of telomerase (Greider and Blackburn, 1985). Details are given in recent review articles by Willard (1990), Blackburn (1991), Greider et al. (1993) and Richards et al. (1993). These findings indicate that there is no theoretical impediment to the occurrence of centric fission. In fact, there is good evidence that fission has occurred in nature (for details see Imai, 1988). Further investigation of the fusion/fission controversy therefore requires assessment of two matters: (1) what are the relative rates of occurrence in nature of fusion versus fission, and which, if either, is predominant?, and (2) what is the biological significance of evolutionary decrease or increase in chromosome number within a lineage?

The minimum interaction theory (Imai et al., 1986) suggests that processes in chromosome number evolution which minimize genetic risk due to deleterious chromosomal interactions, such as reciprocal translocation, might be adaptive. This theory predicts that eukaryotic chromosomal evolution generally involves increase in chromosome numbers due to centric fission. It also recognizes centric fusion as one of the mechanisms serving to eliminate constitutive heterochromatin (C-banding).

The senior author (HTI) has attempted to obtain critical evidence to test the minimum interaction theory by investigating chromosome evolution in ants. To this end, large scale chromosome surveys of Australian formicids were carried out in 1975, 1985, 1987, 1989 and 1991, in an internationally cooperative program involving Japanese and Australian geneticists and myrmecologists, including the authors. Following broad initial studies, the work has concentrated on the

morphologically close-knit complex of species centered on *Myrmecia pilosula* (Fr. Smith) (Subfamily Myrmeciinae). In our previous papers this complex has been indicated nomenclaturally using the aggregate name *Myrmecia (pilosula)*. Relevant specimens in taxonomic collections had been considered by Clark (1951) and Brown (1953) to represent a single, morphologically variable, biological species. These authors did not have genetical information, and the range of specimens available to them was very limited compared to the collections we have assembled. Our findings have conclusively demonstrated that these ants constitute not one species, but a group of morphologically similar sibling species, which vary interspecifically in chromosome number to a remarkable degree. In addition, some of them are intraspecifically chromosomally polymorphic. We recognize at least five cytologically distinct species. Their known chromosome numbers range from $2n = 2$ to $2n = 32$ (Imai, Crozier and Taylor, 1977; Crosland et al., 1988; Imai et al., 1988a; Imai and Taylor, 1989).

In this paper we consider all of the karyological data obtained to date by our surveys, in order to investigate the patterns of chromosome evolution in the *Myrmecia pilosula* species complex, with particular reference to the minimum interaction theory.

2. MATERIALS AND METHODS

Biological materials

A total of 173 colonies of ants referable to the *Myrmecia pilosula* species complex have been collected from 56 localities during our 1975-1991 surveys (for details see Fig. 1). We have used code numbers (see Appendix) of the form HI85-, HI87-, HI89-, and HI91- to indicate colonies collected by H. T. Imai and associates in the relevant seasons from 1985 to 1991 (HI87-30 was, for example, the thirtieth sample collected in 1987). Codes of the form AAGR- and AAGT- apply to colonies collected by Imai in 1975, or by Crozier. The primary voucher specimens are deposited in the Australian National Insect Collection (ANIC), CSIRO, Canberra, with duplicates in the collections of HTI (housed at the National Institute of Genetics (NIG), Mishima 411, Japan) and Masao Kubota (Nakasone 13, Odawara 250, Japan). Taxonomic identifications have been provided by RWT. Formal taxonomic descriptions of the currently unnamed species will be published elsewhere.

Techniques of chromosome preparation

Chromosome preparations were made using prepupal cerebral ganglia, following the improved air-drying technique of Imai et al. (1988a). The preparations were stained with Giemsa (3% in M/15 Sørensen's pH 6.8 phosphate buffer) for 10 min at room temperature. Constitutive heterochromatin (C-bands) may be visualized following air-drying, without treatment by $Ba(OH)_2$. It is difficult to

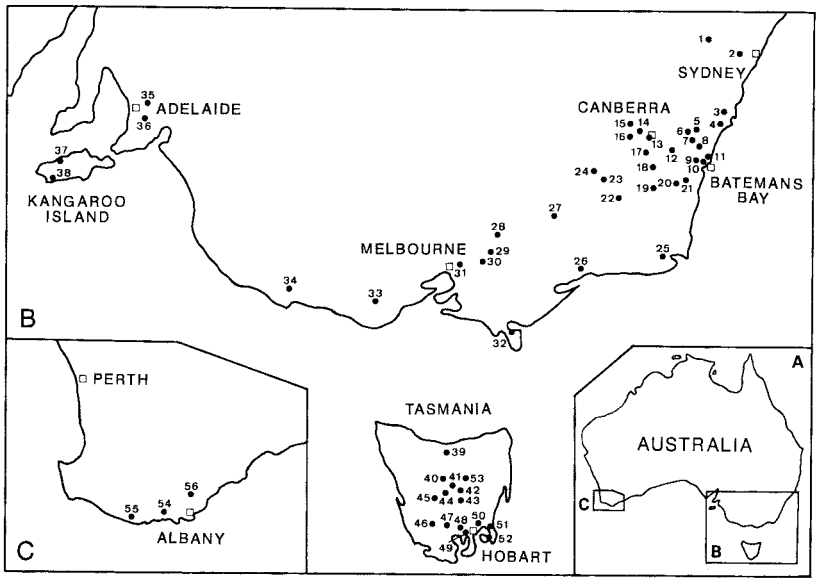

Fig. 1. Locality maps indicating collection sites relevant to this study. A, Reference map of Australia. B, South-east mainland and Tasmania. C, South-west mainland. Open squares, cities or towns, as named. Numbered solid circles, collection sites, as follows (with colony codes in parentheses): 1, Blue Mountains, comprising sites at Lawson (HI87-111-115), Medlow Bath (HI87-116), and Wentworth Falls (HI87-117-121). 2, Leumeah (AAGR-13, AAGT-11). 3, Nowra (HI87-122-127). 4, Wandandian (HI89-034, HI91-48). 5, Corang River Bridge (HI87-136-140, 148-153, HI89-030-032, HI91-49, 50). 6, Mayfield (HI87-154, 155). 7, Charleyong (HI87-156) and Shoalhaven River (HI87-157). 8, Mongarlowe (HI85-192-195, 227-233). 9, West of Nelligen (HI85-213). 10, Sheep Station Creek (HI87-158). 11, Batemans Bay (HI87-160). 12, Captains Flat (HI87-141-145). 13, Canberra (HI85-372, 373, HI87-165, 235, 236, 237). 14, Condor Creek (HI85-376). 15, Picadilly Circus (HI85-373, 374, 375, 378, 379, HI89-033, HI91-51). 16, Tidbinbilla (HI87-146, 147). 17, Gudgenby near Naas Creek (HI87-134, 135). 18, Shannons Flat (HI87-131-133). 19, Wambrook Creek (HI87-128-130). 20, Wadbilliga (HI87-163, 164). 21, Yowrie (HI87-161, 162). 22, Dead Horse Gap (HI87-233, 234, HI91-46, 47). 23, Murray 1 Power Station (HI87-231,232). 24, Cudgewa Bluff Falls (HI87-227-229). 25, West of Genoa (HI89-026-028). 26, Sarsfield (HI89-022-025). 27, Mt. Buffalo (HI87-224-226). 28, Cathedral Range (HI87-222, 223). 29, Marysville, Cumberland Junction (HI87-220,221). 30, Mt. Donna Buang (HI87-219). 31, South Warrandyte (HI87-211-213). 32, Wilson's Promontory (HI87-214-218). 33, South of Colac (HI89-020, 021). 34, North of Heywood (HI89-015, 016). 35, Mt. Lofty (HI87-177, 178). 36, Belair (HI87-181-185). 37, Western River Conservation Park (HI87-170-176). 38, Rocky River (HI87-166-169). 39, North of Latrobe (HI91-39, 40, 42-45). 40, Murderers Hill (HI87-200-202, HI91-25, 26, 28, 33, 34). 41, Miena (HI91-27, 41). 42, 25Km north of Bothwell (HI91-21-23). 43, Bothwell (HI87-197-199). 44, near Derwent Bridge (HI87-207, 208, HI91-35-37). 45, King William Pass (HI87-205, 206). 46, Strathgordon (HI87-193-196). 47, Mt. Weld (HI91-18). 48, Mt. Wellington (HI91-19, 20). 49, Mt. Nelson (HI87-186-188). 50, Granton (HI87-203, 204). 51, Dodges Ferry (HI89-189, 190). 52, Murdunna, Conical Hill (HI87-191, 192, HI91-16, 17). 53, South of Starvegut (HI91-29). 54, North of Denmark (HI89-005, 006, 007, 009, HI91-1, 3). 55, 31km west of Denmark (HI91-8). 56, Prongurup Range (HI91-5).

render G-banding in ants as in other insects, but we have been able to use "chromomere bands" to identify putatively homologous chromosomes. Chromomere bands are often observed in chromosomes at prometaphase, and probably result from regional asynchronism of chromatin condensation. Although banding patterns are not always stable they can nonetheless be used effectively to identify putatively homologous chromosomes in compared metaphase figures.

Nomenclature of chromosome morphology

For this purpose we use the TA$\overline{M}$ system developed by Imai (1991). Chromosomes are classified into three basic categories; telocentric (T), acrocentric (A), and metacentric ($\overline{M}$). T chromosomes are theoretically the ideal chromosome type, and are derived from the $\overline{M}$ category by centric fission. A and $\overline{M}$ chromosomes have the following characteristics:

A: with a heterochromatic short arm and a euchromatic long arm, and $W_s < W_l$.

$\overline{M}$: with both arms euchromatic, and $W_s = W_l$.

where W_s and W_l are the width-ratios of the short and long arms, respectively. We also recognize two special categories of A chromosomes: (1) A^e , being A chromosomes with a euchromatic short arm, and (2) A^M , or pseudoacrocentrics, being A chromosomes with extremely elongate heterochromatic arms. They are characterized as follows:

A^e: both arms euchromatic, and $W_s < W_l$.

A^M: either the short or the long arm heterochromatic, and $W_s = W_l$.

Under the TA$\overline{M}$ system, C-bands located at the pericentromeric, interstitial or terminal regions of chromosome arms are indicated by the codes A^c, A^i, A^t, $\overline{M}^c$, $\overline{M}^i$, $\overline{M}^t$, etc. C-banded chromosomes found in species of the *M. pilosula* complex include A, A^M, A^c, $\overline{M}$, $\overline{M}^t$, $\overline{M}^c$, $\overline{M}^{cc}$, and $\overline{M}^i$ (Fig. 2). To simplify the descriptions we divide these into two groups. The "A-group" includes A, A^M, and A^c chromosomes, and the "$\overline{M}$-group" $\overline{M}$, $\overline{M}^t$, $\overline{M}^c$, $\overline{M}^{cc}$, and $\overline{M}^i$.

Methods for theoretical analysis of chromosome evolution

Because chromosome evolution in the *M. pilosula* species complex is highly complicated, it is difficult to enumerate all the karyotypes examined. We have therefore used methods of statistical analysis in the discussion to follow. The term "chromosome evolution" includes three categories, (1) "karyotype evolution", (2) "chromosome alteration", and (3) evolution of chromosome structure. The former two are categories at the cytological level and the last is at the molecular level. The term "chromosome evolution" is used here as a general term referring (1) and (2). These terms represent distinct, though closely related, concepts. "Karyotype evolution" refers to differentiation of a species-specific chromosome set (karyotype) through speciation. "Chromosome alteration" is defined as the alteration of individual chromosome morphologies in a given taxon, where the relative frequencies of various chromosome types in that taxon are investigated

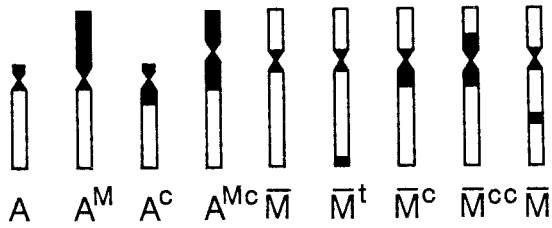

Fig. 2. Schematic representation of C-banded chromosomes observed in *Myrmecia pilosula* species complex. The white sections are euchromatic arms, and the black sections represent constitutive heterochromatin (C-bands). See text and Fig. 4 for detailed definitions of chromosome types.

statistically, as if released from the karyotypes which include them. Thus general tendencies of chromosomal alteration can be visualized. These two concepts are specified here by the karyograph method, and by using chromosomal alteration network analysis. These are briefly outlined below.

The karyograph method

The TA$\overline{\text{M}}$ system of Imai (1991) enables application of the karyograph method of Imai and Crozier (1980) to animals other than mammals. Let 2 K be a diploid karyotype having X_{2n} A-group chromosomes and Y_{2n} $\overline{\text{M}}$-group chromosomes, which is formulated as $2\,\text{K} = X_{2n}\text{A} + Y_{2n}\,\overline{\text{M}}$. In this karyotype, the diploid chromosome number (2n) is $2\text{n} = X_{2n} + Y_{2n}$, and the diploid arm number (2AN, total arm number per diploid karyotype) is given as $2\text{AN} = X_{2n} + 2Y_{2n}$, where euchromatic arms alone (excepting A^{e}) are counted in estimating arm number (i.e., one for each A-group and two for each $\overline{\text{M}}$-group chromosome). Similarly, the haploid karyotypes of male ants are represented as $\text{K} = X_n\text{A} + Y_n\,\overline{\text{M}}$, where the haploid chromosome number (n) and haploid arm number (AN) are respectively $\text{n} = X_n + Y_n$ and $\text{AN} = X_n + 2Y_n$. B-chromosomes (supernumerary chromosomes) are omitted from these expressions because they do not contribute to karyotype evolution.

Using these definitions, a diploid karyotype (2K) can be represented on a two dimensional karyograph by the point corresponding to 2K (2AN, 2n) (Fig. 3). Karyotypes are distributed on the karyograph between the 2K_{A} and $2\text{K}_{\overline{\text{M}}}$ border lines, where $2\text{K}_{\text{A}} = X_{2n}\,\text{A}$ (diploid acrocentric karyotype, $Y_{2n} = 0$) and $2\text{K}_{\overline{\text{M}}} = Y_{2n}$ $\overline{\text{M}}$ (diploid metacentric karyotype, $X_{2n} = 0$). Karyotypes can change their positions on the karyograph due to chromosomal rearrangements which alter their chromosome number (centric fusion or centric fission), or their arm number (A$\overline{\text{M}}$- or $\overline{\text{M}}$A-inversion), or which change both parameters (tandem fusion or tandem fission), where A$\overline{\text{M}}$- or $\overline{\text{M}}$A-inversions are pericentric, changing A chromosomes to $\overline{\text{M}}$ or the reverse.

Karyotypes plotted on the karyograph conserve the numerical information on chromosomal rearrangements which have been recorded in karyotypes either as

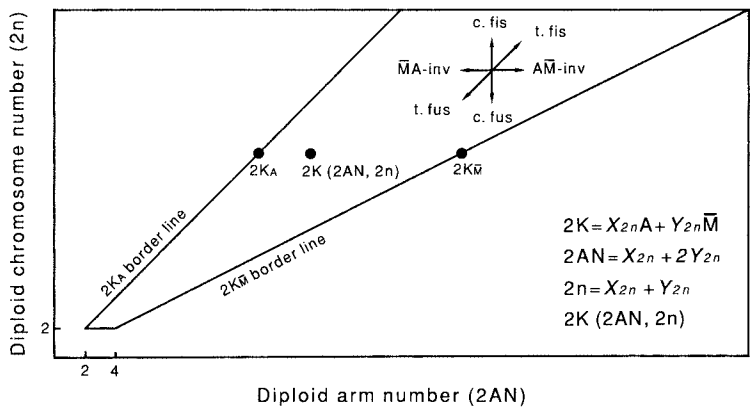

Fig. 3. Karyographic representation of a diploid karyotype (2K) and directions of movement on the karyograph resulting from centric fusion (c. fus), centric fission (c. fis), AM̄-inversion (AM̄-inv), M̄A-inversion (M̄A-inv), tandem fusion (t. fus), and tandem fission (t. fis). $2K_A$ and $2K_{\bar{M}}$ represent diploid acrocentric and metacentric karyotypes, respectively. X_{2n} and Y_{2n} indicate diploid numbers of acrocentric (A) and metacentric (M̄) chromosomes. See text for details.

chromosome number (n or 2n) or as arm number (AN or 2AN) during the course of evolution. Although the karyograph method is not always useful for reconstructing the karyotypic phylogeny of a given taxon, the distribution patterns of karyotypes on the karyograph conserve information concerning the overall directionality of karyotype evolution in such a taxon. Further details are given in later sections.

Chromosomal alteration network analysis

The prototype formulation of network analysis was proposed by Imai (1978, 1991) as "cyclical chromosome change". A brief outline of the steps needed for the construction of networks is:

Step 1: The A- and M̄-group chromosomes are distinguished, and the chromosome types of each group are arranged in the order of their frequencies.

Step 2: The chromosome rearrangements and accompanying morphological alterations in the A- and M̄- groups are listed. Centric fission (c. fis), centric fusion (c. fus), AM̄-inversion (AM̄-inv), addition (C^+) or deletion (C^-) of constitutive heterochromatin, and shift of centromere activity (sft) are the major rearrangements known in ants (Fig. 4).

(1) $1\bar{M} - (c.\ fis) \rightarrow 2T - (C^+) \rightarrow 2A$ (Fig. 4a),
(2) $2A - (c.\ fus) \rightarrow 1\bar{M}$ (Fig. 4b),
(3) $1A - (A\bar{M}\text{-inv}) \rightarrow 1\bar{M}^t - (C^-) \rightarrow 1\bar{M}$ (Fig. 4c),
(4) $1A - (C^+) \rightarrow 1A^M$ (Fig. 4d),
(5) $2A^M - (c.\ fus) \rightarrow 1\bar{M}^c$ (Fig. 4e),
(6) $1A^M - (A\bar{M}\text{-inv}) \rightarrow 1\bar{M}^{ct} - (C^-) \rightarrow 1\bar{M}^c$ (Fig. 4f),

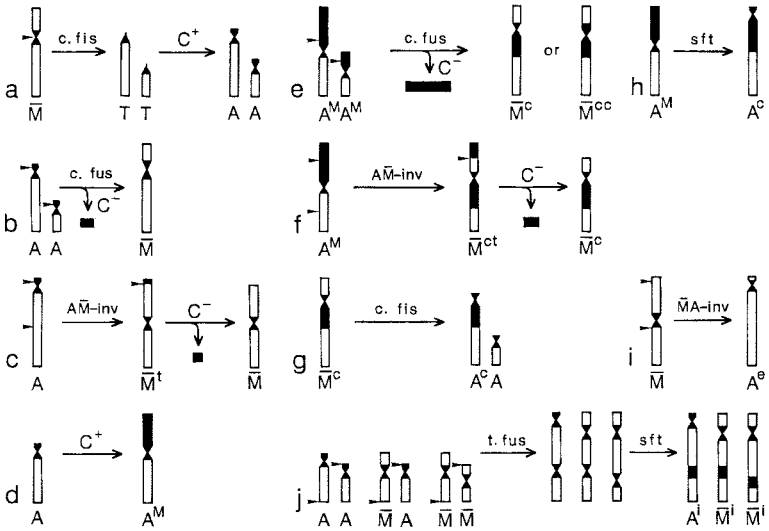

Fig. 4. Chromosomal rearrangements theoretically expected or actually observed in ants. See Fig. 2, for details of chromosome-morphology nomenclature. a and g, Centric fission. b and e, Centric fusion. c and f, A$\bar{M}$-inversion. d, Formation of pseudoacrocentric (A^M) by addition of constitutive heterochromatin (C^+). h, Shift of centromere activity. i, $\bar{M}$A-inversion. j, Tandem fusions accompanying shift of centromere activity. The black parts of centromeres are C-bands. Arrowheads indicate breakage sites in each rearrangement. Constrictions within C-bands indicate the centromeres.

(7) $1\bar{M}^c - (\text{c. fis}) \rightarrow 1A^c + 1A$ (Fig. 4g),
(8) $1A^M - (\text{sft}) \rightarrow 1A^c$ (Fig. 4h),
(9) $2A^M$ or $2A^c - (\text{c. fus}) \rightarrow 1\bar{M}^{cc}$ (Fig. 4e),
(10) $1\bar{M} - (\bar{M}\text{A-inv}) \rightarrow 1A^e$ (Fig. 4i), and
(11) 2A or $1A + 1\bar{M}$ or $2\bar{M} - (\text{t.fus} + \text{sft}) \rightarrow 1A^i$ or $1\bar{M}^i$ (Fig. 4j).

Step 3: Construction of the networks. The chromosome alterations (1), (2), and (3) indicated above form a closed network, which is termed the primary network. In the same way, (4)–(9) and (10)–(11) respectively form the secondary and tertiary networks. The primary and secondary networks are connected by the alterations numbered (4) and (7). The secondary network originates from A^M chromosomes, and the endproducts by centric fusion or A$\bar{M}$-inversion always accompany C-band insertion ($\bar{M}^c$, $\bar{M}^{cc}$). The tertiary network includes minor derivatives from the primary or secondary networks resulting from C^+ (A^i, $\bar{M}^i$, etc.) or $\bar{M}$A-inversion (A^e). Examples of each network are shown in Fig. 16.

Step 4: Each chromosomal alteration is ranked by the frequencies of the end products involved, and is represented by dotted arrows (< 1%), broken arrows (1–5%), and solid arrows with various thicknesses corresponding to the frequencies involved. The resulting visual presentation effectively demonstrates the

general flow of chromosome alterations in the taxon under examination.

3. OBSERVATIONS

A. Chromosomes, morphologies, and geographical distributions in the Myrmecia pilosula *species complex*

M. pilosula (Smith) is a small-sized species of the primitive Australian genus *Myrmecia*. Its nomenclatural holotype was collected in Tasmania early last century. This ant is commonly referred to as the "Jack-jumper" because of its hopping behavior when disturbed. *M. pilosula* usually builds a small nest-mound on the ground in open *Eucalyptus* forest or at road sides, and the mound is decorated with small pebbles, gum nuts and fragments of carbon etc. Before we began our study, numbers of specimens more-or-less similar to the *pilosula* holotype had been collected in Tasmania, south eastern mainland Australia and southernmost Western Australia, and they had been identified more-or-less consistently in museum collections and publications as *M. pilosula*-that is as specimens putatively conspecific with the *pilosula* holotype (see Clark, 1951; Brown, 1953, Browning, 1987). Our surveys have revealed that these specimens, and the many series which we have subsequently collected, represent at least five independent, very similar or sibling species, namely: *M. pilosula* (Fr. Smith, 1858)(=*Ponera ruginoda* Fr. Smith, 1858); *M. croslandi* Taylor, 1991; *M. imaii* Taylor; *M. banksi* Taylor and *M. haskinsorum* Taylor. Taylor's taxonomic analysis includes formal descriptions and nomenclature of the last three species. In case the present work at publication antedates his report, we here expressly declare that the information given below concerning these taxa is not intended to account for their formal taxonomic description. Any implied nomenclatural priority over the Taylor paper is specifically denied - it is not intended, nor should it be construed. Detailed karyological data of these species are summarized in Appendix. Further details concerning each species are:

M. croslandi: The first karyologically-studied colony of *M. croslandi* was collected by M. W. J. Crosland at Tidbinbilla, Australian Capital Territory (ACT) in 1985. This remarkable species has the lowest chromosome number known among animals, namely $2n=2$ (Crosland and Crozier, 1986). We have subsequently located many colonies in various parts of Canberra (ACT), at Corang River Bridge, Mayfield and the nearby Shoalhaven River in the Braidwood district of New South Wales (NSW), and one from South Warrandyte, near Melbourne, Victoria (Vic). This species is distinguished from others by its robust form and other details (Taylor, 1991). It builds a small flat nest mound without decoration.

We have demonstrated that *M. croslandi* in fact varies in chromosome number, with $2n=2$, 3 or 4, and that it has highly complicated chromosome polymorphisms, including telomere fusion, shift of centromeric activity by centromeric

inactivation, saltatory growth of constitutive heterochromatin (C^+), and $A\overline{M}$-inversion. These karyological details have been reviewed by Imai and Taylor (1989). Before being formally named by Taylor (1991) *M. croslandi* had been discussed as *M. pilosula* by Crosland and Crozier (1986), and as *M.* (*pilosula*) $n = 1$ by Imai and Taylor (1989). Typical *croslandi* karyotypes with $2n = 2$ ($2K = 2\overline{M}^{ci}$) and $2n = 3$ ($2K = 1A^c + 1\overline{M} + 1\overline{M}^{ci}$) are illustrated here (Figs 5a and 5b).

M. imaii: This species is geographically very isolated from all other taxa of the *pilosula* species complex, and has a very distinctive karyotype. It is found only in the Albany/Denmark area of extreme southern Western Australia. Eight colonies have been analyzed from three sites (54, 55, and 56 in Fig. 1 and Appendix). The basic karyotype, $2K = 6A + 2A^M$ ($2n = 8$), is quite different from those of other species discussed here. Two independent $A\overline{M}$-inversions were found on chromosomes 1 and 2 (Figs 5c-g). Every step of $A\overline{M}$-inversion ($A \rightarrow \overline{M}^t \rightarrow \overline{M}$) has been conserved as a polymorphism in chromosome 1 (A, Fig.

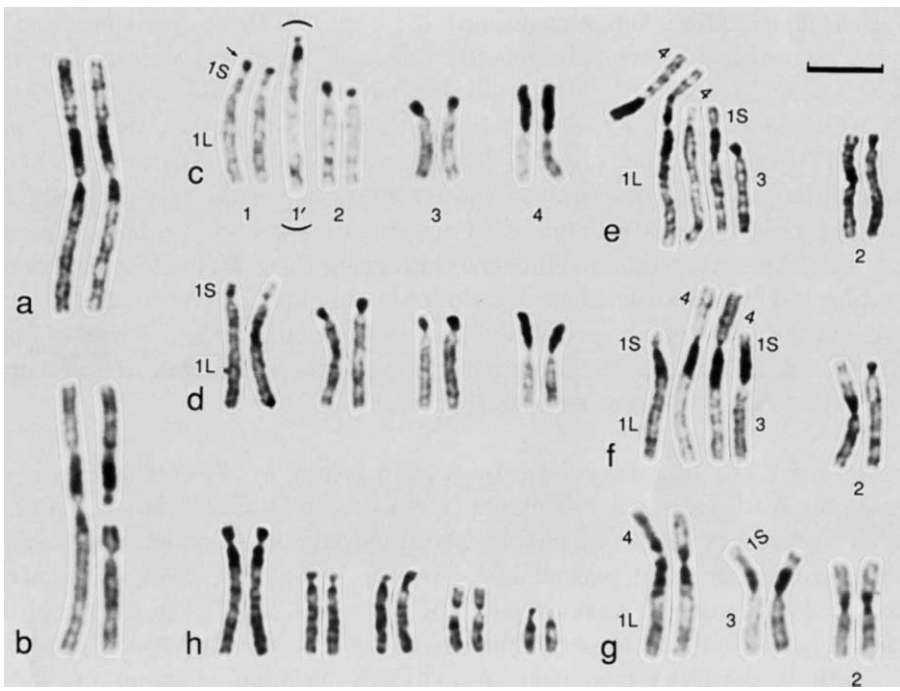

Fig. 5. C-banded karyotypes of *Myrmecia croslandi* (a and b), *M. imaii* (c-g), and *M. banksi* (h). 1S and 1L are the short and long arms of chromosome 1 in *M. imaii*. Chromosome 1 of *M. imaii* showed polymorphism involving $A\overline{M}$-inversion. Three chromosome types, acrocentric (1' in parentheses), metacentric with a terminal cap ($\overline{M}^t$, small arrow in c-1), and metacentric without a terminal cap ($\overline{M}$) were observed. Whole arm transpositions between 1L and chromosome 4 and between 1S and chromosome 3 were also found (e-g). Scale bar represents 5 μm.

5c-1' in parenthesis; $\overline{M}^t$, an intermediate with a terminal heterochromatin cap indicated by an arrow in Fig. 5c-1; $\overline{M}$, the terminal cap was lost in Fig. 5d-1S). In the case of chromosome 2, the heterochromatic short arm of acrocentric (A) is inserted as pericentromeric heterochromatin in the metacentric induced by A$\overline{M}$-inversion ($\overline{M}^c$, Figs 5e-g). Complicated chromosome polymorphisms accompanying chromosome number reduction ($2n = 8 \rightarrow 7 \rightarrow 6$) by A$\overline{M}$-inversion, centric fission and centric fusion were observed between chromosomes 1L and 4 and between chromosomes 1S and 3 (Figs 5e-g). Despite this chromosomal complexity we consider all specimens examined here to be conspecific.

M. banksi: We have encountered this relatively distinctive species at low-lying localities along the east coast of NSW between Sydney and Batemans Bay (locality codes 2, 3, 4, 9, 10, 11 in Fig. 1). It is easily recognized within the *pilosula* species complex by the brassy-green pubescence which characteristically adorns its head, and by a monomorphic karyotype $2K = 6\overline{M} + 2\overline{M}^c + 2A$ ($2n = 10$) (Fig. 5h), which characterizes all specimens examined except one mutant individual with a complicated translocation ($2n = 9$, AAGH-11, Imai, Crozier and Taylor, 1977). *M. banksi* is morphologically similar to *M. imaii*, but *Imaii* lacks heavy cephalic pilosity, and has a very distinctive karyotype as mentioned above. This species has been referred to in previous papers as the "greenhead" form of *M.* (*pilosula*), or as *M.* (*pilosula*) $2n = 10$.

M. haskinsorum: We first found this distinctive species in Tasmania (HI87-197-200, HI91-27, 41; locality codes 40, 41, 43). It frequently has deep indigo blue body reflections, dark-colored legs, and characteristically, an almost total absence of pilosity on the head, mesosoma and petiole. We subsequently found *haskinsorum* near Corang River Bridge, NSW, (HI87-152; loc. code 5), at Mt. Buffalo, Vic, (HI87-224, 225; loc. code 27), and at Dead Horse Gap (HI87-233, 234, HI91-46, 47; loc. code 22) in the Snowy Mountains, NSW. These records imply that the species is distributed mainly on mountains at elevations exceeding 1,000 m.

Chromosome numbers vary in *M. haskinsorum* between $2n = 12$ and $2n = 24$ (Appendix, Fig. 6). This range results mainly from centric fission, centric fusion, and A$\overline{M}$-inversion. The karyotypes of colonies from Corang River Bridge and Mt. Buffalo, with $2n = 23/24$ and $2n = 20$, respectively (Figs 6a and 6b), are closely related to those from Tasmania with $2n = 18$ (Fig. 6c). The Dead Horse Gap colonies, on the other hand, have $2n = 18/15/12$ (Figs 6e-h), and are karyotypically more similar to a Tasmanian colony with $2n = 17$ (Fig. 6d). Four fusions with different arm combinations were detected from colony HI87-234 (Fig. 6h).

M. pilosula: We have identified *M. pilosula* by consulting its holotype in the Natural History Museum, London, U.K. It was previously collected near

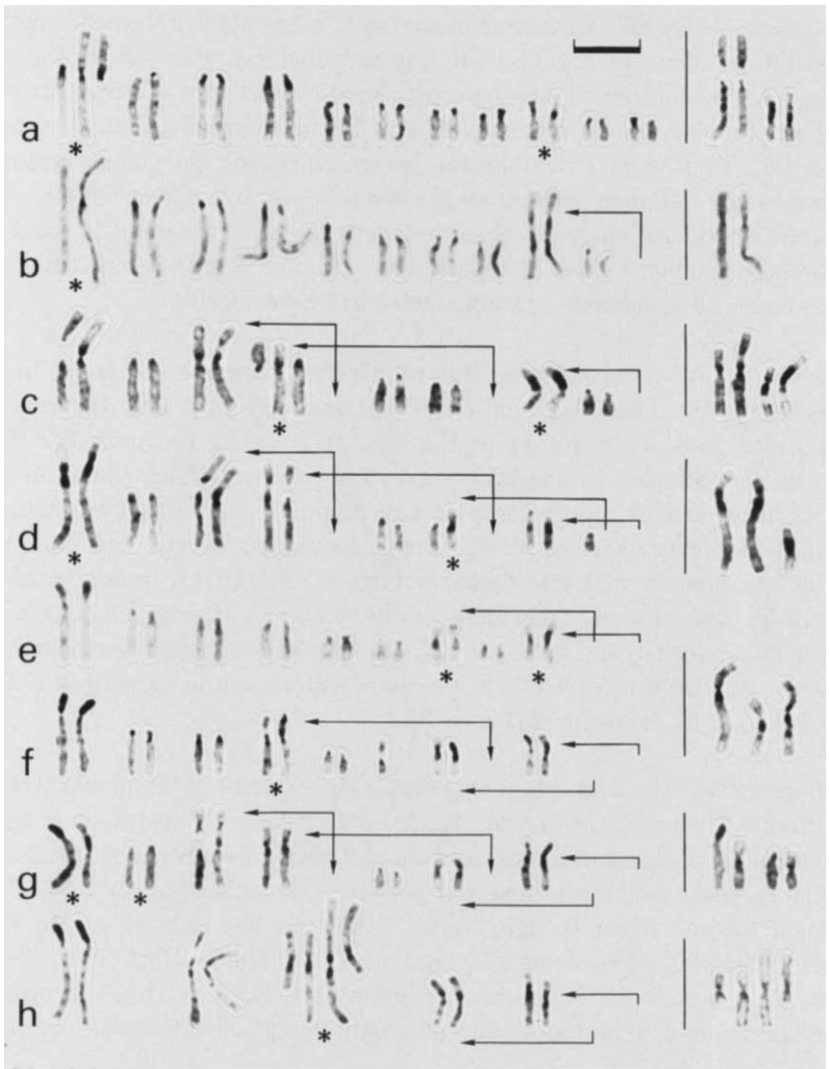

Fig. 6. C-banded karyotypes of *Myrmecia haskinsorum*. a, 2n = 23 (HI87-152; Corang River Bridge, collection site 5 in Fig. 1). b, 2n = 20 (HI87-224; Mt. Buffalo, site 27). c, 2n = 18 (HI87-197; Bothwell, site 43). d, 2n = 17 (HI87-197; Bothwell, site 43). e-h, Dead Horse Gap (site 22): e, 2n = 18 (HI87-233); f, 2n = 15 (HI87-233); g, 2n = 15 (HI91-46); h, 2n = 12 (HI87-234). Chromosomes indicated by asterisks are shown in duplicate at right, beyond the vertical lines. Arrows indicate acrocentric chromosomes involved in each centric fusion. The scale bar represents 5 μm.

Hobart, where the species can be locally very common. Within its species complex *pilosula* is relatively small and gracile, with unexceptional pilosity.

In this paper we use the name *M. pilosula* in two senses: (1) *M. pilosula* s. lat. (= sensu lato, or "broad sense", referring to all specimens we have studied referable to the *pilosula* species complex, but excluding those classified as *M.*

banksi, *M. croslandi*, *M. haskinsorum*, *M. imaii*, and putative F_1 to be discussed below). This s. lat. category probably comprises several sibling biological species which we are unable at present to distinguish or define with confidence. (2) *M. pilosula* s. str. (= sensu stricto, or "strict sense", referring to those specimens which are closely morphologically similar to the holotype of *M. pilosula* and are considered to be biologically conspecific with it).

Myrmecia pilosula s. lat. is distributed on the continental mainland along the Great Dividing Range in New South Wales and Victoria and westwards across the southern coasts of Victoria and South Australia (SA). It is the only taxon of the

Fig. 7. C-banded karyotypes of *Myrmecia pilosula* s. str. showing fission burst. a, 2n = 23 (HI87-193; Strathgordon, collection site 46 in Fig. 1). b, 2n = 23 (HI87-194; Strathgordon, site 46). c, 2n = 24 (HI87-187; Mt. Nelson, site 49). d, 2n = 26 (HI87-188; Mt. Nelson, site 49). e, 2n = 23 (HI87-168; Rocky River, site 38). f, 2n = 24 (HI87-182; Belair, site 36). g, 2n = 27 (HI89-015; North of Heywood, site 34). Chromosomes indicated by asterisks are shown in duplicate at right, beyond the vertical lines. Arm combination of eight pairs of metacentrics are always constant in these polymorphic karyotypes, indicating fission polymorphism. The scale bar represents 5 μm.

pilosula species complex known from SA. There are several color variants. One of them has bright red, more-or-less uniformly-colored legs. Other forms have sections of the legs colored dark or blackish-brown. The red-legged form is known only from Kangaroo Island (SA), Adelaide (SA), Colac (Vic), Heywood (Vic) and southeastern Tasmania (see locality codes 33–53 in Fig. 1). Colonies of this form, which we recognize as *M. pilosula* s. str. can include individuals with remarkable fission polymorphisms (Fig. 7), especially in Tasmania. Details are given below.

Our karyological results suggest that some entities in the *pilosula* species complex possess hybrid karyotypes, implying that any "good" sibling species present might have originated from hybridization events. This view is supported by HTI who considers that some of the karyotypes have probably resulted from hybridization between elements classified here as *M. pilosula* s. lat. and *M. banksi*. They have $2n = 15$, 18, or 19 (Fig. 8). The subject specimens were taken from colonies collected along or near the Princes Highway between Batemans Bay, NSW, and Canberra (Fig. 9, solid stars; locality codes 6, 7, 13, and 21 in Fig. 1; also, see Appendix). All individuals examined include a haploid karyotype of *banksi*-type $K = 1A + 2\overline{M} + 2\overline{M}^c$ and one of *pilosula*-type (compare Figs 5h and 8). These forms are denoted by Imai as PBF_1 (pilosula-banksi F_1). PBF_1s are generally referable to *M. pilosula* s. lat. on morphological grounds, but the color patterns of their legs differ from those of other populations, and could be considered intermediate between *pilosula* s. str. and *M. banksi* (Fig. 10). Taylor does not believe that these color differences necessarily demonstrate the hybri-

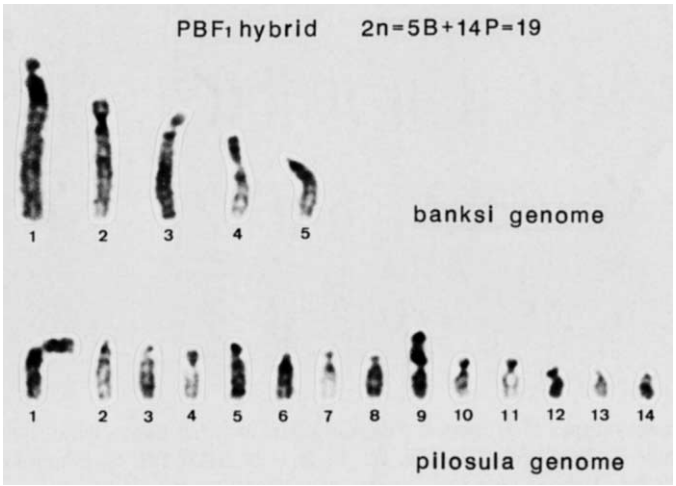

Fig. 8. A C-banded karyotype of a putative PBF_1 hybrid (*pilosula-banksi* F_1) with $2n = 5B + 14P = 19$ (HI85-372; Canberra, collection site 13 in Fig. 1). This karyotype includes genome sets from *M. banksi* (five chromosomes of top row, $n = 5B$) and *M. pilosula* s. lat. (14 chromosomes in the bottom row, $n = 14P$). See Fig. 5h for banksi karyotype.

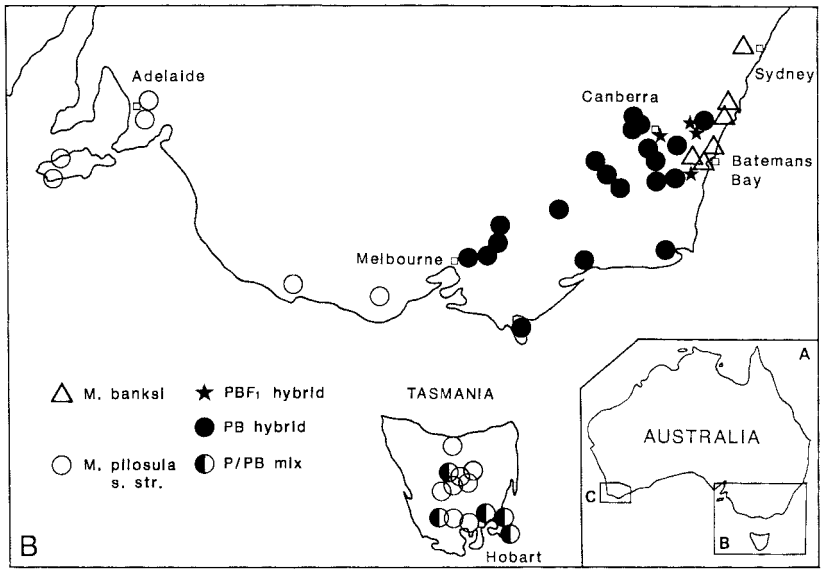

Fig. 9. Geographical distribution of *M. banksi* (open triangles), *M. pilosula* s. str. (open circles), their putative hybrid PBF_1 hybrid with F_1 karyotype (stars), back-cross PB-hybrids between PBF_1 and *pilosula* s. lat. (solid circles), and P/PB mix mixed colonies (divided circles).

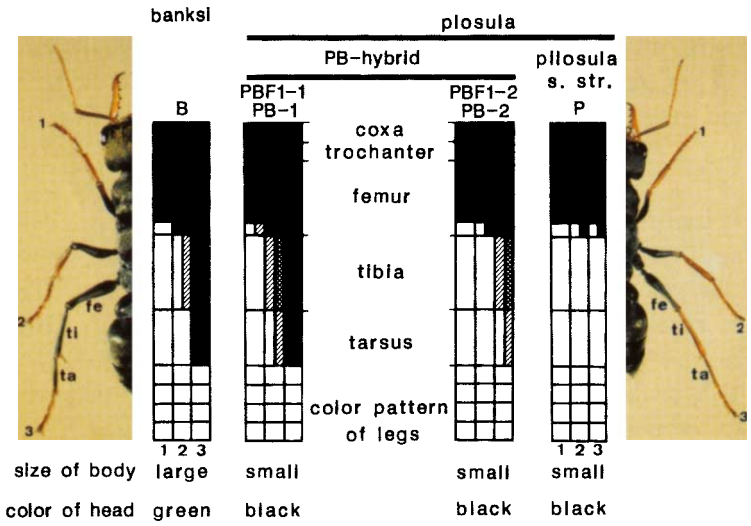

Fig. 10. Color patterns of the legs in *M. pilosula* s. str. (P), *M. banksi* (B) and their putative hybrids (PB-hybrid, PB-1, PB-2, FBF_1-1 and FBF_1-2).

dization proposed by Imai on karyological grounds. Imai inclines also to subdivide PBF_1 into two types, PBF_1-1 and -2, based on the color patterns of their legs, where the former is more similar to the *banksi* configuration than the latter. Taylor argues that the differences in coloration of the legs could result from natural selection operating differently in different places, perhaps related to different assemblages of small *Myrmecia* species (including *croslandi* and *haskinsorum*) encountered sympatrically by *pilosula* s. lat. across its range. Leg-coloration in other *Myrmecia* species is known to vary geographically in this way, either by character displacement between otherwise similar species, or due to mimetic resemblance between the sympatric forms.

Sampled karyotypes from a number of colonies collected in the Great Dividing Range (locality codes 1, 5, 8, 12-32 in Fig. 1; see Appendix) are considered by Imai to be PB-hybrids. They are karyotypically like *pilosula* s. str. ($2n = 22 - 30$; see Appendix), and no chromosomes putatively related to those of *banksi* have been detected (Fig. 11). The color patterns of the legs of voucher specimens from the same nests as karyotyped individuals are similar to those of PBF_1 (Fig. 10). Most of these karyotypes are similar to PBF_1-1, but six colonies from Corang River Bridge (locality code 5) and Wadbilliga (locality code 20) were of PBF_1-2 type. These are denoted PB-1 and PB-2, respectively. As will be discussed later, these PB-hybrids are considered by Imai possibly to represent back-crosses between PBF_1 and *pilosula* s. str. In contrast to *pilosula* s. str. PB-hybrids evidence fusion polymorphisms accompanying saltatory increases of constitutive heterochromatin (C^+) (Figs 11a-d), a matter discussed in more detail below.

Some unusual Tasmanian colonies in which *pilosula* s. str. and PB-1 or -2 individuals are mixed (locality codes 40, 42, 46, 50, 51, and 52) have been observed. They generally accord karyotypically with *pilosula* s. str., but appear to have been genetically influenced by contact with elements like the mainland PB-hybrids.

B. Fission and fusion polymorphisms in M. pilosula *s. lat.*

Excepting PBF_1 hybrids with $2n = 15$ or 19, chromosome numbers of *M. pilosula* s. lat. range between $2n = 18$ and $2n = 32$ (see Appendix). This numerical variation results mainly from Robertsonian rearrangement. However, the observed forms of polymorphism are quite different when *pilosula* s. str. and the putative PB-hybrids are compared; the former exhibits fission polymorphism, and the latter fusion polymorphism. Details follow:

Fission polymorphism in pilosula *s. str.*: The common karyotype of *M. pilosula* s. str. in Tasmania comprises nine basic chromosome pairs, of which five pairs of metacentrics show centric fission polymorphism (Figs 7a-d). Fission polymorphism can be distinguished from fusion polymorphism because it involves a constant (fixed) arm combination in each metacentric involved in the Robertsonian poly-

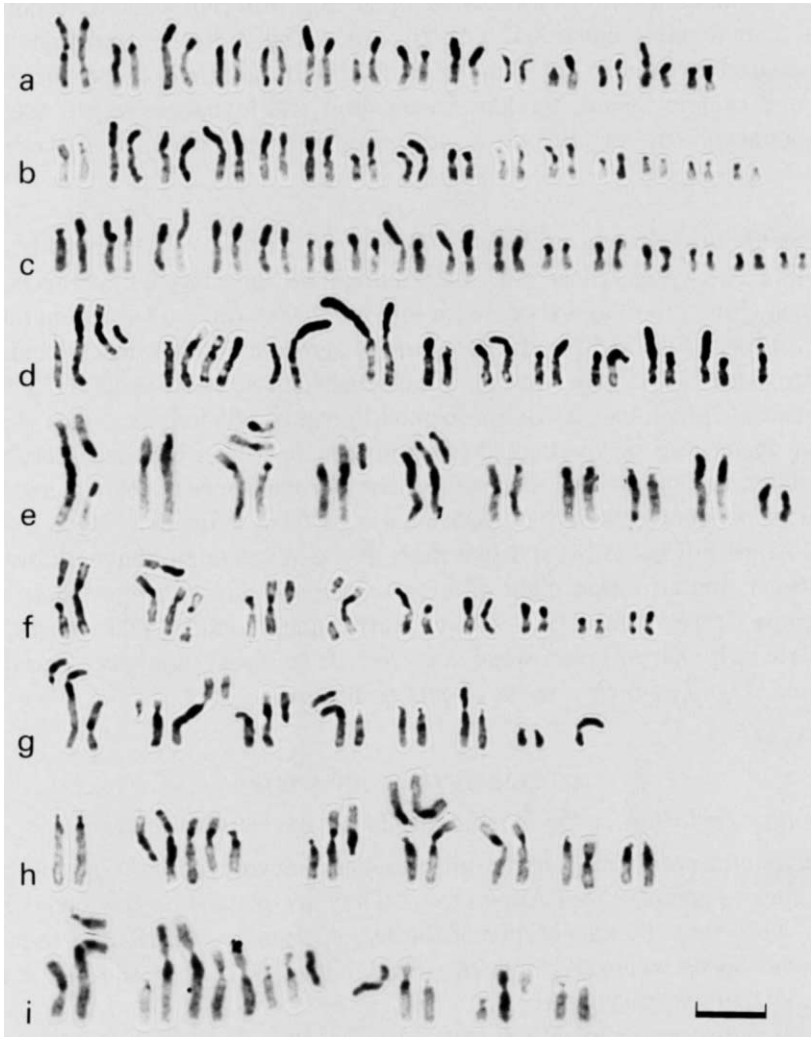

Fig. 11. C-banded karyotypes of putative PB-hybrids. a, 2n = 28 (HI87-130; Wambrook Creek, collection site 19 in Fig. 1). b, 2n = 30 (HI87-219; Mt. Donna Buang, site 30). c, 2n = 32 (HI87-141; Captains Flat, site 12). d, 2n = 25 (HI87-116; Medlow Bath, site 1). e, 2n = 25 (HI87-140; Corang River Bridge, site 5). f, 2n = 24 (HI87-146; Tidbinbilla, site 16). g, 2n = 20 (HI87-121; Wentworth Falls, site 1). h, 2n = 20 (HI87-163; Wadbilliga, site 20). i, 2n = 19 (HI87-121; Wentworth Falls, site 1). The scale bar represents 5 μm.

morphism. In Figs 7a-d, each of the first six metacentrics illustrated has the same arm combination in the karyotypes obtained from different individuals. These metacentrics are dissociated by centric fission within individuals, so that 14 different karyotypes were detected in cells from 11 individuals of the three colonies HI87-186-188 (Tasmanian locality code 49 in Fig. 1 and Appendix). In

the same population, three karyotypes including different centric fissions were obtained from a single individual with $2n = 24$. This indicates that fissioning can occur repeatedly, even in the same individual. In addition to such fission polymorphisms, centric fusion, tandem fusion, and $A\overline{M}$-inversion were observed as minor polymorphisms in *pilosula* s. str. samples from mainland Australia (Figs 7e-g).

Fusion polymorphism in putative PB-hybrids: Putative PB-hybrids can be divided into two types, those with high-numbered ($2n = 28 - 32$) acrocentric-rich karyotypes (Figs 11a-c) and those with low-numbered ($2n = 19 - 26$) metacentric-rich karyotypes (Figs 11d-i). In the former, acrocentrics frequently change into pseudoacrocentrics (A^M) by addition of heterochromatic short arms (C^+). In the latter, most of the metacentrics are formed by centric fusion.

Centric fusion can be distinguished from centric fission by the heterobrachial arm combinations of each of the metacentric chromosomes involved, and by the insertion of pericentromeric heterochromatin to form C-bands. Note the insertion of C-bands in Figs 11d-i, and that most of the metacentrics have different arm combinations, and also, that eight different chromosomes exchanged their arms in an extreme case (Fig. 11i). These karyological data indicate that the metacentric-rich karyotypes were derived from high-numbered acrocentric karyotypes (Figs 11a-c) by a burst of centric fusions.

4. THEORETICAL ANALYSIS

A. Karyotype evolution in the Myrmecia pilosula *species complex*

We have observed 192 polymorphic diploid karyotypes in taxa of the *M. pilosula* species complex (see Appendix). They are plotted on the karyograph in Fig. 12. Note that the karyotypes of the five species are distributed themselves without overlap between $2K_A$ and $2K_{\overline{M}}$ border lines (enclosing the loci of diploid acro- or metacentric karyotypes).

Based on the rearrangements detected in this species complex (see Appendix), some possible pathways of karyotype evolution in *croslandi*, *imaii*, *banksi*, and *haskinsorum* are indicated in Fig. 12 by small arrows. (The situation of *M. pilosula* s. lat. will be discussed shortly). The directions of arrows in Fig. 12 imply that tandem fusion and centric fusion are predominant in these species.

There is, however, an alternative scenario (involving a statistical approach) for explanation of the gross directionality of karyotype evolution of these ants.

Types (and frequencies) of rearrangements detected in the *pilosula* species complex are: centric fission (112), centric fusion (79), $A\overline{M}$-inversion (52), $\overline{M}A$-inversion (0), tandem fusion (7), and tandem fission (10) (see Appendix). These data indicate that centric fission, centric fusion, and $A\overline{M}$-inversion are the major rearrangements in these ants, while $\overline{M}A$-inversion and tandem fusion are neglig-

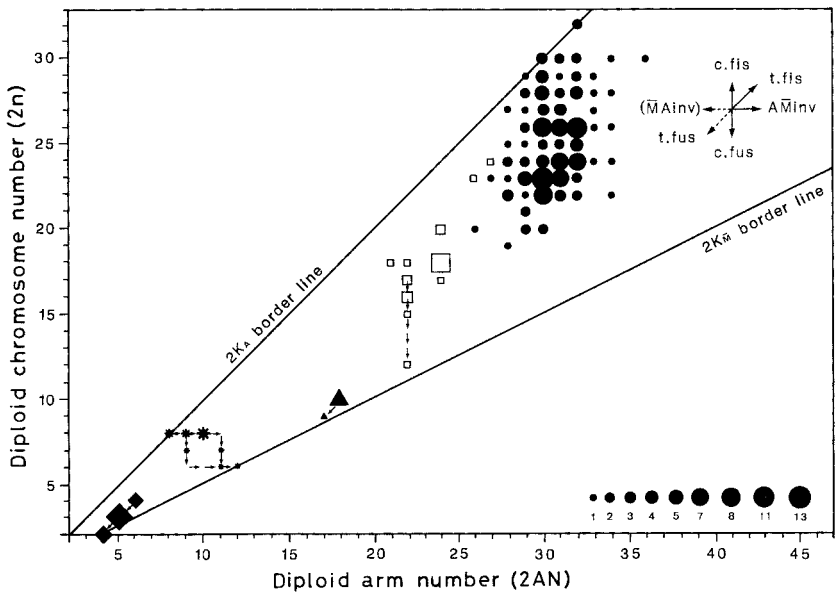

Fig. 12. Karyotypes of taxa of the *Myrmecia pilosula* species complex in karyographic representation. Solid diamonds, *M. croslandi*. Asterisks, *M. imaii*. Solid triangles, *M. banksi*. Open squares, *M. haskinsorum*. Solid circles, *M. pilosula* including *M. pilosula* s. str. (P) and putative PB-hybrids. Small arrows indicate directionality of karyotype evolution observed in this study. See Fig. 3 for explanation of karyograph methodology. Numerals attached under the solid circles at lower right indicate the number of karyotypes represented at appropriate loci on the graph.

ibly rare or at most minor. Tandem fission is in practical terms a result of AM̄-inversion and centric fission (for details see Imai, 1993).

The alternative solution is then that the karyotypes of members of the *pilosula* species complex have been evolving generally toward increases in arm number (2AN) or chromosome number (2n) by AM̄-inversion or by centric fission ($2n = 4 \rightarrow 32$), with frequent but temporary reductions of chromosome numbers by centric or tandem fusion. The reverse alteration ($2n = 32 \rightarrow 4$) is quantitatively unlikely, because of the rarity of M̄A-inversion and tandem fusion. This means that karyotypes cannot move easily on the karyograph to the left (by M̄A-inversion) or lower left (by tandem fusion). If the karyotype 2K = 32A evolves towards reducing chromosome number, two possible mechanisms could be involved: (1) centric fusion and M̄A-inversion ($2K = 32A - (16$ c. fus$) \rightarrow 16\bar{M} - (16\bar{M}$A-inv$) \rightarrow 16A - (8$c. fus$) \rightarrow 8\bar{M} - (8\bar{M}$A-inv$) \rightarrow 8A - (4$c. fus$) \rightarrow 4\bar{M} - (4\bar{M}$A-inv$) \rightarrow 4A$); or (2) tandem fusion ($2K = 32A - (28$ t. fus$) \rightarrow 4A$). We need to assume, in both cases, a total of 28 M̄A-inversions or tandem fusions, which would be remotely likely, considering the evidence we have obtained. Karyotype evolution of each of these species is discussed further in a later section.

B. Fission and fusion burst in M. pilosula *s. lat.*

A cluster of centric fissions was found in *M. pilosula* s. str. populations in Tasmania (Figs 7 and 13a-b), which we denote as "fission burst". Likewise, we found "fusion burst" in putative PB-hybrids on the mainland (Figs 11 and 13c-d).

Centric fusion ($2A \rightarrow 1\overline{M}$) and centric fission ($1\overline{M} \rightarrow 2T \rightarrow 2A$) are both Robertsonian rearrangements, but opposite in direction. It is usually difficult to distinguish between the two except by the arm combinations of metacentrics involved in a particular polymorphism. The arm combinations of metacentrics differ from the original in a fusion polymorphism (being heterobrachial), but the original combinations are conserved in fission polymorphism (being homobrachial; see Fig. 5 in Imai, 1993). In this connection, C^+ chromosomes such as A^M, A^c, $\overline{M}^c$, or $\overline{M}^{cc}$ seem to be valuable markers for detecting centric fusion in ants, because they are theoretically induced from A chromosomes as follows; $A-(C^+) \rightarrow A^M-$(c. fus) $\rightarrow \overline{M}^c$ or $\overline{M}^{cc}$ (Figs 4d-e).

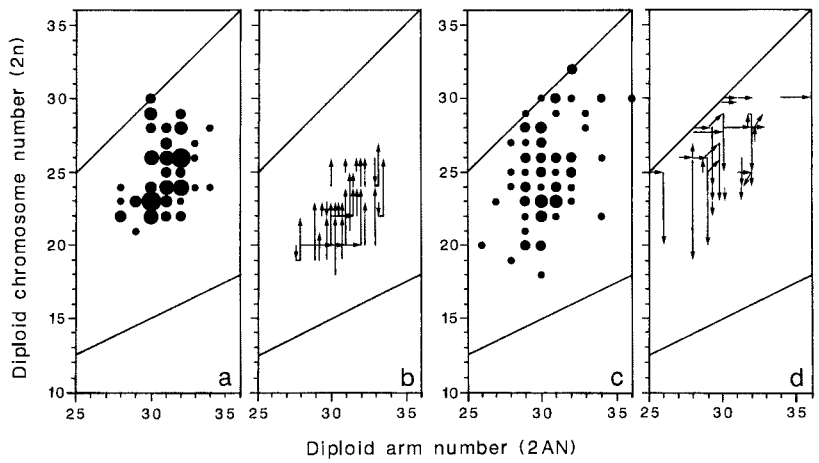

Fig. 13. Karyographic presentation of fission burst (a, b) and fusion burst (c, d) found in *M. pilosula* s. str. and putative PB-hybrids. Arrows indicate directionality of karyotype evolution.

Frequencies (%) of C-banded (C^+) chromosomes in populations at each of our localities are shown in a contour map in Fig. 14. Note that populations with fission burst show very low values - below 30% (compare open circles in Fig. 9 and dotted areas in Fig. 14). On the other hand, frequencies exceed 50% along the Great Dividing Range, and this corresponds with the hypothecated PB-hybrid zone (compare solid circles in Fig. 9 and shaded areas in Fig. 14). Our work has revealed that constitutive heterochromatin is associated nonspecifically in the interphase nuclei of C-band-rich karyotypes (Fig. 15). The biological meaning of this will be discussed below.

The evidence that the fusion burst appeared preferentially in the PB-hybrid

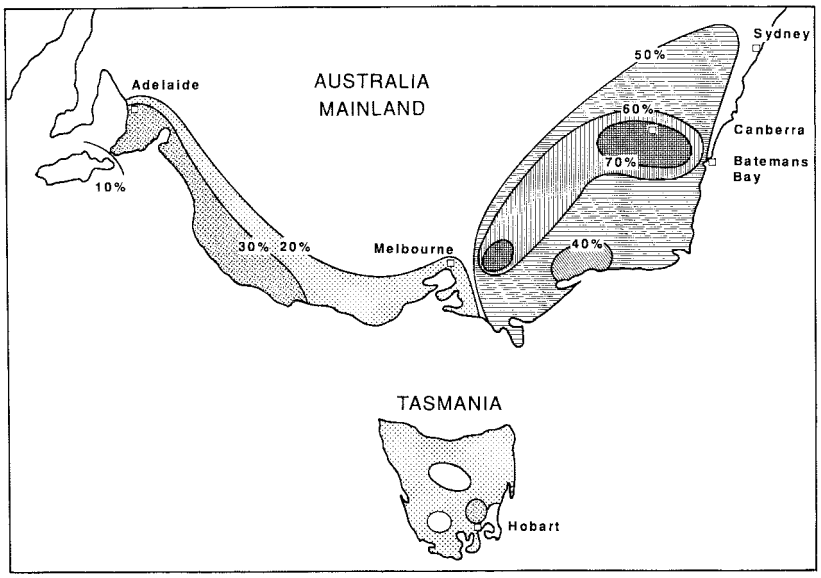

Fig. 14. Geographic distribution of *Myrmecia pilosula* with frequencies (%) of C-band-bearing chromosomes (A^M, $\overline{M}^c$ or $\overline{M}^{cc}$ etc.) per karyotype.

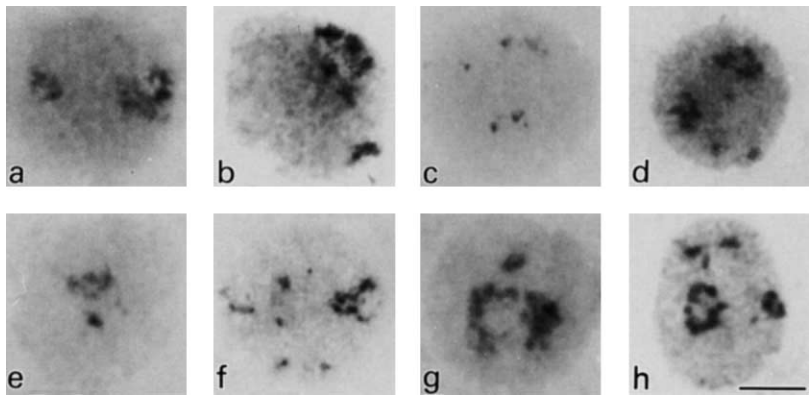

Fig. 15. Nonspecific association of constitutive heterochromatin (C-bands) in interphase nuclei of taxa of the *Myrmecia pilosula* species complex. a, *M. croslandi* (2n = 3, HI91-49, Fig. 5b). b, *M. imaii* (2n = 8, HI91-1, Fig. 5c). c, *M. banksi* (2n = 10, HI91-48, Fig. 5h). d, *M. haskinsorum* (2n = 18, HI87-197, Fig. 6c). e, *M. haskinsorum* (2n = 23, HI87-152, Fig. 6a). f, *M. pilosula* s. str. (2n = 23, HI87-194, Fig. 7b). g, putative PB-hybrid (2n = 32, HI87-141, Fig. 11c). h, PB-hybrid (2n = 25, HI87-116, Fig. 11d). The scale bar represents 5 μm.

zone, which is characterized by a high incidence of C-banded (C^+) chromosomes (A^M or $\overline{M}^c$ in Figs 11 and 14), suggests strong causal relationships between interspecific hybridization (elements of *pilosula* s. lat. × *banksi*), saltatory

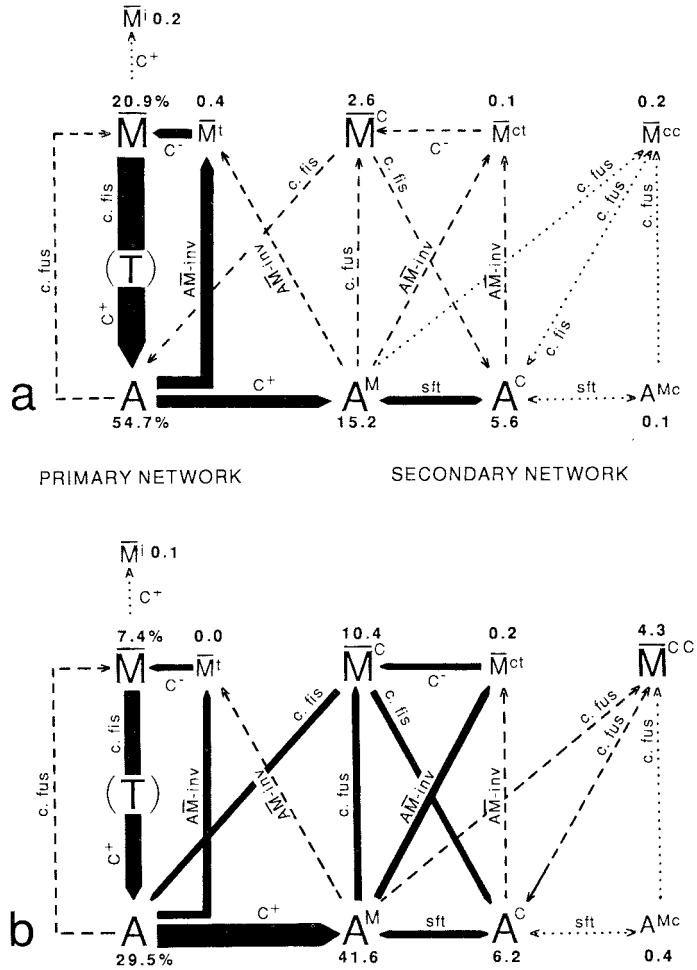

Fig. 16. Chromosomal alteration network analysis of *Myrmecia pilosula* s. str. with fission burst (a) and putative PB-hybrids with fusion burst (b). For chromosome nomenclatures see Fig. 2. The primary network is predominant in *M. pilosula* s. str. (a), but the role of the secondary network increases in PB-hybrids (b).

growth of heterochromatic short arms of acrocentrics ($A-(C^+)\rightarrow A^M$), and the fusion burst (A^M-(c. fus)$\rightarrow \bar{M}^c$ or $\bar{M}^{cc}$). Chromosomal alteration network analysis provides valuable information towards the solution of this matter, as follows.

C. Chromosomal alteration network analysis in M. pilosula *s. str.*

The chromosomal alteration networks of *pilosula* s. str. and the putative PB-hybrids are represented in Figs 16a and b. The net frequency of chromosomes involved in the primary and secondary networks is 76.0% and 23.8% in the former, and 36.9% and 63.1% in the latter. The primary network predominates

over the secondary in *pilosula* s. str. but the reverse occurs in PB-hybrids.

The primary network consists of two linked cycles: the fission-inversion cycle ($M-$(c. fis)$\rightarrow T-(C^+)\rightarrow A$ -(AM-inv)$\rightarrow \overline{M}$); and the fission-fusion cycle ($\overline{M}-$(c. fis)$\rightarrow T-(C^+)\rightarrow A-$(c. fus)$\rightarrow \overline{M}$). The latter is rarely present in *M. pilosula* s. str., because most of the centric fusions detected in that species accompanied C-band insertion ($\overline{M}^c$ or $\overline{M}^{cc}$, i.e., components of the secondary network) (Fig. 4e). This means that the chromosome evolution of *pilosula* s. str. proceeds as a whole toward increasing chromosome number by centric fission and A$\overline{M}$-inversion (the primary network) with temporary reductions of chromosome number by centric fusion (the secondary network). This evolutionary pattern is applicable to the ants in general (Imai, 1991).

On the other hand, the importance of the secondary network increases significantly in PB-hybrids (Fig. 16b). This is due mainly to an extraordinary increase in the frequency of A^M chromosomes (15.2% $\rightarrow$ 41.6%) due to addition of constitutive heterochromatin ($A-(C^+)\rightarrow A^M$) (Fig. 4d) and a decrease in the frequency of A chromosomes (54.7% $\rightarrow$ 29.5%). A similar network pattern has been observed also in bees and wasps, which are also taxa of the order Hymenoptera) (Hoshiba and Imai, 1993). The frequency of centric fusion accompanying C-band insertion (A^M-(c. fus)$\rightarrow \overline{M}^c$ or $\overline{M}^{cc}$) (Fig. 4e) in the secondary network of PB-hybrids increases about 4 times (12.8%) above that in the primary network (3.2%), constituting the fusion burst.

In connection with this model Imai (1988, 1991) proposed that centric fusion could be one of the mechanisms for eliminating the constitutive heterochromatin of A^M chromosomes, where $\overline{M}^c$ or $\overline{M}^{cc}$ chromosomes are considered to be fusion derivatives (Figs 4e and f). Our results show that, in the fusion burst in PB-hybrids, the constitutive heterochromatin of A^M (Figs 11a-c) is mostly eliminated in the metacentrics ($\overline{M}^c$ or $\overline{M}^{cc}$) induced by centric fusion (Figs 11d-i), though such elimination is not always complete, and heterochromatin blocks are inserted in M^c or M^{cc} chromosomes as pericentromeric C-bands. The increase of A^M chromosomes in PB-hybrids remains to be explained. A likely possibility is the introduction of an instability in acrocentrics (A) induced by interspecific hybridization.

D. A possible phylogeny of M. pilosula *species complex*

We have considered elsewhere that the lowest-numbered ($2n=2$) karyotype $2K=2\overline{M}^{ci}$ of *M. croslandi* is derived secondarily from a hypothetical ancestral karyotype $2K=4A^M$ ($2n=4$) by tandem fusion and A$\overline{M}$-inversion (Imai and Taylor, 1989). The other known low-numbered karyotype in *Myrmecia* is that of *M. piliventris* ($2K=4\overline{M}^c$) (HI85-172). This has also been interpreted as a derivative of $2K=4A^M$ by two A$\overline{M}$-inversions (Imai et al., 1988a). We suggest that the hypothetical karyotype $2K=4A^M$ could be ancestral in *Myrmecia*, and that *M. croslandi* could be close in this regard to the stem-species of the *pilosula* complex.

From this stem species, *M. imaii* (2n = 6 – 8), *M. banksi* (2n = 9, 10), and *M. pilosula* s. lat. (2n = 18 – 32) could have been differentiated more-or-less successively. These three species have greenish-gold hairs on the head (where they are much thicker in *banksi* than in the other two taxa). *M. pilosula* s. lat. is also smaller in average size, and more gracile than *banksi*. We consider these two species to be closely related on grounds of general morphological similarity. Also, if Imai's hypotheses are correct, they are able to hybridize to produce PBF_1 or PB-hybrids, perhaps further indicating close relationship between them. On the other hand, *M. haskinsorum* (2n = 12 – 24) seems possibly to have branched independently from a *croslandi*-like ancestor. It is morphologically the most distinctive known species of the complex. A possible phylogeny of the *M. pilosula* species complex, based mainly on cytogenetic considerations developed in this paper, and relevant references cited here, is given in Fig. 17.

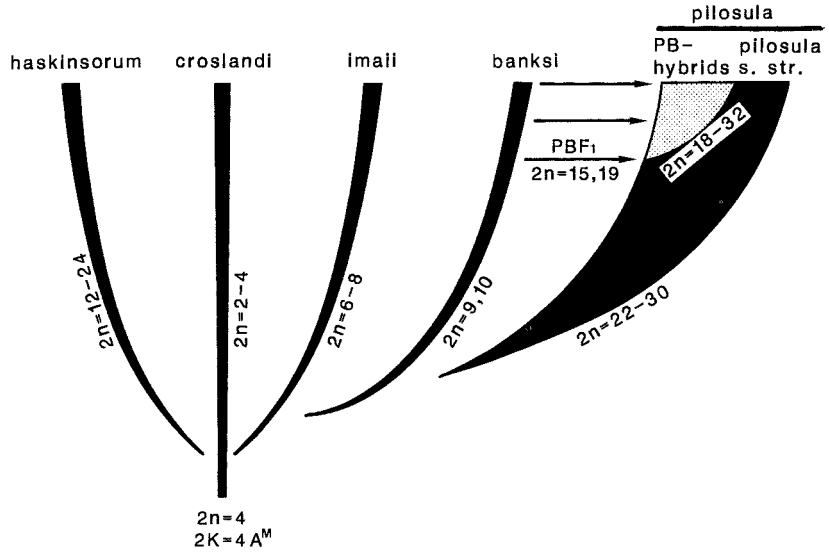

Fig. 17. A possible phylogeny of *Myrmecia pilosula* species complex with indication of relevant chromosome numbers.

Because each of the species of the *M. pilosula* species complex is karyologically so distant from the others (Fig. 12), chromosomal homologues cannot be discerned with confidence. Even the various PBF_1-hybrids are distinct, separated by their parental karyotypes, because chromosomes of *banksi* origin have never been found in PB-hybrid karyotypes (see discussion below for further details). The fact that each species except *banksi* has complex chromosomal polymorphisms indicates that each chromosome rearrangement, such as centric fusion, centric fission and $A\bar{M}$-inversion, itself does not initiate speciation in the *pilosula* species complex, but rather they seem to work in combination.

5. DISCUSSION

A. Chromosome evolution in the Myrmecia pilosula *species complex, with reference to the minimum interaction theory*

The minimum interaction theory (Imai et al., 1986) was developed in order to clarify the fusion/fission controversy in chromosome evolution. We here discuss chromosome evolution in the *Myrmecia pilosula* species complex in light of the minimum interaction theory, and propose that some cytological data deriving from our studies provide supporting evidence for the theory.

Basic assumptions of the minimum interaction theory: The minimum interaction theory relies on three basic assumptions: (1) that chromosomal interactions accompanying DNA exchanges at pachytene are important for chromosome evolution, (2) that these chromosome interactions are induced by the crossing-over mechanism or by mis-resolution following chromosomal interlocking, and (3) that chromosomal interactions are non-random due to the hammock structure (a configuration of bivalents at pachytene resulting from the attachment of their terminals on the inner surface of the nuclear membrane).

Theoretical analyses using these assumptions require karyotypic evolution to proceed towards the minimization of chromosomal interactions capable of inducing deleterious translocations. They predict that increase in chromosome numbers by centric fission would be adaptive for this purpose. Centric fusion and A$\overline{\text{M}}$-inversion operate to diminish constitutive heterochromatin (C-bands) which would increase rapidly after centric fission, because of instability in telocentric chromosomes.

Supporting evidence for the minimum interaction theory found in studies of the Myrmecia pilosula *species complex and other ants*: Most of the cytological evidence discussed here was obtained from processed somatic cells of worker ants, which are genetically female but subfertile. The data can, however, be used to consider cytological events which would or might have occurred in germ cells of related fertile female, queen, ants. The results are summarized as follows:

(1) Centric fission, A$\overline{\text{M}}$-inversion, and centric fusion are the three major chromosomal rearrangements found in the *Myrmecia pilosula* species complex (see Appendix), as in other ants (Imai et al., 1988a). A high incidence of centric fission polymorphisms, here termed the "fission burst", was observed in *M. pilosula* s. str. in Tasmania (Figs 7 and 13a-b).

(2) Telocentrics (T) induced from metacentrics ($\overline{\text{M}}$) by centric fission are unstable, and promptly change into acrocentrics (A) or pseudoacrocentrics (A^M) by saltatory increase of constitutive heterochromatin (C^+). No telocentrics (T) were observed by us in karyotypes heterozygotes for centric fission (1$\overline{\text{M}}$/2T), instead, A or A^M or A^c chromosomes were detected (1$\overline{\text{M}}$/2A, A^M or A^c, Fig. 7).

(3) The C-banded chromosomes (A^M, A^c, $\overline{M}^c$, or $\overline{M}^{cc}$) appeared frequently (50-70%/karyotype) in the putative interspecies hybrids between *M. pilosula* s. lat. and *M. banksi* (Fig. 14).

(4) Nonspecific associations of C-bands in interphase nuclei were observed in C-band-rich karyotypes (Fig. 15), in which case the chromosomes were physically close to each other.

(5) A unique phenomenon, "fusion burst" (Figs. 11d-i, 13c-d) was observed preferentially in the putative interspecific hybrids between *M. pilosula* s. lat. and *M. banksi* (Fig. 9).

(6) The amount of constitutive heterochromatin (present as C-bands) was reduced in the $\overline{M}^c$- or $\overline{M}^{cc}$-bearing karyotypes induced by the fusion burst (Figs 11d-i) compared to the A^M-rich karyotypes (Figs 11a-c), suggesting that centric fusion is a mechanism for C-band elimination.

(7) In addition to centric fusion, A$\overline{M}$-inversion is a C-band elimination-mechanism. The direct end-products of A$\overline{M}$-inversion ($\overline{M}^t$ or $\overline{M}^{ct}$) necessarily have a terminal cap of constitutive heterochromatin (A or $A^M - (A\overline{M}\text{-inv}) \rightarrow \overline{M}^t$ or $\overline{M}^{ct}$) (Figs 4c and f), but the end-products actually observed are $\overline{M}$ or $\overline{M}^c$ chromosomes, which would be expected following the elimination of the terminal caps ($\overline{M}^t$ or $\overline{M}^{ct} - (C^-) \rightarrow \overline{M}$ or $\overline{M}^c$) (Figs 4c and f). The intermediate $\overline{M}^t$ or $\overline{M}^{ct}$ chromosomes have been found in *M. imaii* (Fig. 5c), *Myrmecia. sp. cf. fulvipes* and *M. nigrocincta* (see Figs 2a-k of Imai, Crozier and Taylor, 1977).

(8) Deleterious chromosomal rearrangements such as translocations were observed frequently in *pilosula*-group species with low chromosome numbers ($2n < 24$), but rarely in the high-numbered species ($24 \leqq 2n \leqq 94$) (Imai, Crozier and Taylor, 1977; Imai et al., 1988a).

(9) Karyotype evolution in the *M. pilosula* species complex proceeds as a whole toward an increase in chromosome numbers ($2n = 4 \rightarrow 2n = 32$). This conclusion is based upon both karyograph analysis (Fig. 12) and chromosomal alteration network analysis (Fig. 16).

The way in which these items in evidence contribute to the minimum interaction theory is now discussed.

Basic modes of chromosome evolution under the minimum interaction theory: As indicated above in the methods section, the term chromosome evolution is used in this paper generally to include both karyotype evolution and chromosomal alteration. Fig. 18 represents the relationship between the two concepts. In that figure, karyotypes are illustrated as bivalents at pachytene (i.e., haploid karyotype K), a stage at which they are arranged nonrandomly to form a hammock structure. To simplify discussion, the chromosomal alteration network shown in Fig. 16 is modified in Fig. 18 (minor alterations are omitted or combined into one category, and the primary and secondary networks are arranged symmetrically). We discuss here some basic pathways of chromosome evolution expected

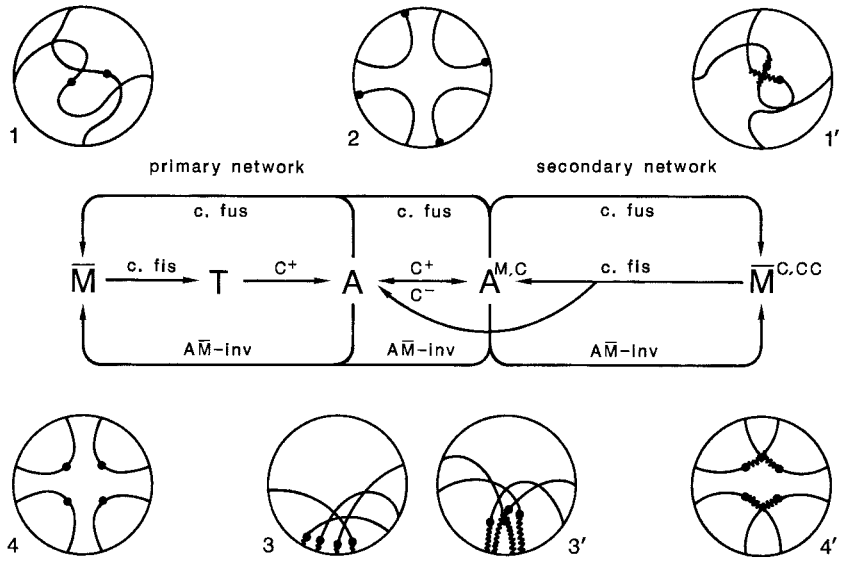

Fig. 18. Schematic representation of chromosome evolution in *Myrmecia pilosula* species complex, following precepts of the minimum interaction theory. The term 'Chromosome evolution' is used generally to include both karyotype evolution and chromosome alteration. Karyotypes are represented by chromosomes in interphase nuclei (circles), at which point they are distributed nonrandomly, with their terminals attached to the inner surface of the nucleus (i.e., arranged in the 'hammock structure'). Constitutive heterochromatin (in C-bands) is indicated by zigzag lines. Solid circles indicate centromeres. 1, $K_{2\overline{M}}$ (or $K=2\overline{M}$). 1', $K_{2\overline{M}^{c,cc}}$ ($K=2\overline{M}_{c,cc}$). 2, K_{4T} ($K=4T$). 3, K_{4A} ($K=4A$). 3', K_{4A^M} ($K=4A^M$). 4, $K_{4\overline{M}}$ ($K=4\overline{M}$). 4', $K_{4\overline{M}^{c,cc}}$ ($K=4\overline{M}^{c,cc}$). "Chromosome alteration" refers to morphological alterations of individual chromosomes ($\overline{M}$, T, A, $A^{M,c}$, $\overline{M}^{c,cc}$), which form closed cycles (the primary and secondary networks). The chromosomal alteration networks indicated here are modified from those shown in Fig. 16. See text for further details, and Figs 2 and 4 for nomenclature of chromosomes and chromosome rearrangements.

in a situation where genome size (except for C-banding) and nuclear volume are constant (we have preliminary data of the *M. pilosula* species complex).

Let $K_{2\overline{M}}$ be a haploid karyotype with two metacentric chromosomes (Fig. 18-1). Similarly let K_{4T} (Fig. 18-2) and K_{4A} (Fig. 18-3) indicate respectively a telocentric and an acrocentric haploid karyotype, where the size of each chromosome is smaller than that in $K_{2\overline{M}}$. $K_{4A^{M,c}}$ (Fig. 18-3') and $K_{4\overline{M}^{c,cc}}$ (Fig. 18-4') indicate karyotypes comprising A^M or A^c, and $\overline{M}^c$ or $\overline{M}^{cc}$ chromosomes, respectively.

Now, starting from the $K_{2\overline{M}}$ configuration, four basic modes of chromosome evolution are possible:

(a) $K_{2\overline{M}} - (\overline{M} - (\text{c. fis}) \rightarrow T) \rightarrow K_{4T} - (T - (C^+) \rightarrow A) \rightarrow K_{4A}$
$- (A - (A\overline{M}\text{-inv}) \rightarrow \overline{M}) \rightarrow K_{4\overline{M}}$ (Figs 18-1 → 2 → 3 → 4),

(b) $K_{2\overline{M}} - (\overline{M} - (\text{c. fis}) \rightarrow T) \rightarrow K_{4T} - (T - (C^+) \rightarrow A^M) \rightarrow K_{4A^M}$
$- (A^M - (A\overline{M}\text{-inv}) \rightarrow \overline{M}^{c,cc}) \rightarrow K_{4\overline{M}^{c,cc}}$ (Figs 18-1 → 2 → 3' → 4'),

(c) $K_{2\overline{M}} - (\overline{M} - (\text{c. fis}) \rightarrow T) \rightarrow K_{4T} - (T - (C^+) \rightarrow A) \rightarrow K_{4A}$

$- (A - (c.\ fus) \rightarrow \overline{M}) \rightarrow K_{2\overline{M}}$ (Figs 18-1 → 2 → 3 → 1), and

(d) $K_{2\overline{M}} - (\overline{M} - (c.\ fis) \rightarrow T) \rightarrow K_{4T} - (T - (C^{+}) \rightarrow A^{M}) \rightarrow K_{4A^{M}}$
$- (A^{M} - (c.\ fus) \rightarrow \overline{M}^{c,cc}) \rightarrow K_{2\overline{M}^{c,cc}}$ (Figs 18-1 → 2 → 3' → 1'),

where $K_{2\overline{M}} \rightarrow K_{4T} \rightarrow K_{4A} \rightarrow K_{4\overline{M}}$ are stages in pathways of karyotype evolution, and the chromosomal alterations and rearrangements contributing to each step are shown in parentheses.

The endproduct $K_{4\overline{M}}$ (Fig. 18-4) is theoretically the most stable karyotype involved, because potential chromosome interactions are minimal in this case. $K_{4\overline{M}^{c,cc}}$ (Fig. 18-4') is slightly unstable because of C-banding instability. The other karyotypes are also unstable, because chromosomal interactions increase with increasing chromosome size ($K_{2\overline{M}}$, Fig. 18-1; $K_{2\overline{M}^{c,cc}}$, Fig. 18-1'), due to saltatory increase of C-banding due to telomere instability (K_{4T}, Fig. 18-2), or by nonspecific association of C-bands generating C-banding instability (K_{4A}, Fig. 18-3 or $K_{4A^{M,c}}$, Fig. 18-3').

Under these restrictions evolutionary modes (a) and (b) are effective for the minimization of chromosomal interactions, though (b) is slightly unstable due to C-banding instability. On the other hand, (c) and (d) are only makeshift as evolutionary mechanisms providing escape from C-banding instability, because the end-products ($K_{2\overline{M}}$ and $K_{2\overline{M}^{c,cc}}$) are subject to the same difficulties as the starting karyotype ($K_{2\overline{M}}$), as discussed above. Their fate is to restart the process.

In $K_{4\overline{M}}$ of chromosome evolution mode (a), if $\overline{M}$ chromosomes still interact the karyotype will evolve again as $K_{4\overline{M}} \rightarrow K_{8T} \rightarrow K_{8A} \rightarrow K_{8\overline{M}}$ (or $K_{4\overline{M}}$). Therefore, in the long term, karyotypes can be expected to evolve toward increasing chromosome numbers until chromosome interactions are minimized.

Our model system assumes that all chromosomes in a given karyotype change synchronously by way of the same type of chromosome rearrangements. However, each chromosome in a given karyotype has the potential to change independently of the others, and to undergo different rearrangement. Thus in practice, more complicated modes of chromosome evolution than those discussed above would be expected. In fact, in the case of the *Myrmecia pilosula* species complex, it is almost impossible to trace past processes with any real confidence in order to reconstruct karyotype phylogeny. Karyotype evolution can thus only be described statistically, based on the mass distribution of karyotypes on the karyograph (Fig. 19).

Modes of mass karyotype evolution under the minimum interaction theory: Patterns of mass karyotype evolution on the karyograph differ in relationship to the starting karyotypes $2K_{\overline{M}}$ and $2K_A$, and in the relative rates for centric fission, centric fusion, and $A\overline{M}$-inversion. In the case of the $2K_{\overline{M}}$ karyotypes, three basic patterns on the karyograph would be expected (see also Fig. 4);

(1) upward movement due to fission burst, i.e., c. fis $\gg A\overline{M}$-inv $\approx$ c. fus ≈ 0 (Fig. 19a-1),

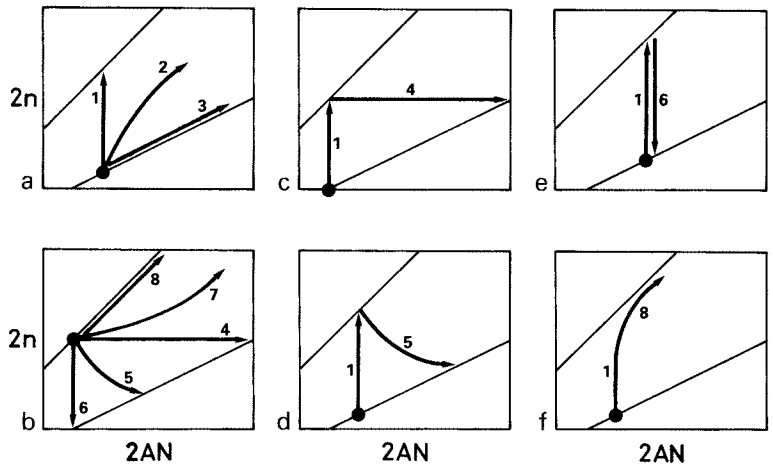

Fig. 19. Patterns of mass karyotype evolution following the precepts of the minimum interaction theory. Directionality of karyotype evolution on the karyograph is determined by relative evolutionary rates of centric fission (c. fis), centric fusion (c. fus) and A$\overline{\text{M}}$-inversion (A$\overline{\text{M}}$-inv). a, Patterns starting from a $2K_{\bar{M}}$ karyotype: a-1, c. fis $\gg$ A$\overline{\text{M}}$-inv $\approx$ c. fus ≈ 0. a-2, c. fis $\approx$ A$\overline{\text{M}}$-inv $>$ c. fus. a-3, A$\overline{\text{M}}$-inv $>$ c. fis $\gg$ c. fus. b, Patterns starting from $2K_A$. b-4, A$\overline{\text{M}}$-inv $\gg$ c. fis $\approx$ c. fus ≈ 0. b-5, c. fus $\approx$ A$\overline{\text{M}}$-inv $>$ c. fis. b-6, c. fus $\gg$ A$\overline{\text{M}}$-inv $\approx$ c. fis ≈ 0. b-7, c. fis $\approx$ A$\overline{\text{M}}$-inv $>$ c. fus. b-8, c. fis $>$ AM-inv $\gg$ c. fus. c, Compound pattern (1+4). d, (1+5). e, (1+6). f, (1+8). See text for details and also Fig. 3.

(2) to the right and upward if c. fis $\approx$ AM-inv $>$ c. fus (Fig. 19a-2),

(3) upward along the $2K_{\bar{M}}$ border line if A$\overline{\text{M}}$-inv $>$ c. fis $\gg$ c. fus (Fig. 19a-3).

In the same way, five modes are potentially possible in the case of $2K_A$ karyotypes (see also Fig. 4):

(4) to the right by inversion burst, i.e., A$\overline{\text{M}}$-inv $\gg$ c. fis $\approx$ c. fus ≈ 0 (Fig. 19b-4),

(5) to the right and downward if c. fus $\approx$ A$\overline{\text{M}}$-inv $>$ c. fis (Fig. 19b-5),

(6) downward by fusion burst, i.e., c. fus $\gg$ A$\overline{\text{M}}$-inv $\approx$ c. fis ≈ 0 (Fig. 19b-6),

(7) to the right and upward if c. fis $\approx$ A$\overline{\text{M}}$-inv $>$ c. fus (Fig. 19b-7), and

(8) upward along the $2K_A$ border line if c. fis $>$ A$\overline{\text{M}}$-inv $\gg$ c. fus (Fig. 19b-8).

Of the above alternatives, (1), (4), (5) and (6) terminate evolution when the $2K_A$ or $2K_{\bar{M}}$ karyotypes are induced, but the other enumerated modes continue to increase chromosome number indefinitely along the $2K_{\bar{M}}$ border line (3) or the $2K_A$ border line (8), or in an intermediate manner (2, 7). In any case, the relative rate for each rearrangement is assumed to be constant, and the expected karyotype distribution patterns are linear.

If the evolutionary rates fluctuate with time and from species to species compound patterns will appear, resulting from different combinations of the basic patterns mentioned in the previous section. For example: (1 + 4) (Fig. 19c), (1 + 5) (Fig. 19d), (1 + 6) (Fig. 19e), and (1 + 8) (Fig. 19f). The first three begin

from $2K_{\bar{M}}$ by fission burst and end with $2K_A$, at which point $A\bar{M}$-inversion and/or centric fusion come into operation, but at different rates, e.g., $A\bar{M}$-inv $\gg$ c. fus in $(1+4)$, $A\bar{M}$-inv $\simeq$ c. fus in $(1+5)$, and c. fus $\gg A\bar{M}$-inv (fusion burst) in $(1+6)$.

The compound pattern $(1+4)$ is the combination of the basic mode (a) or (b) mentioned in the previous section, where centric fission and $A\bar{M}$-inversion alternate. Therefore, by repeating this $(1+4)$ pattern karyotypes would evolve along an upwardly zigzag course between the two border lines. This is the course likely to be most favored by selection for minimizing chromosomal interaction. On the other hand, the compound pattern $(1+5)$ is less efficient for increasing chromosome number. In the compound pattern $(1+6)$, the fission and fusion bursts alternate. This course is the least effective option, as mentioned in basic modes (c) or (d), because the genetical advantage of centric fission is completely disrupted by centric fusion. Finally, the compound pattern $(1+8)$ is expected if metacentrics ($\bar{M}$) induced by $A\bar{M}$-inversion change rapidly by centric fission into acrocentrics.

Based on these theoretical analyses, mass karyotype evolution in the *Myrmecia pilosula* species complex is rediscussed below.

Modes and rates of the mass karyotype evolution in the Myrmecia pilosula *species complex*: In Fig. 20, various pathways of karyotype evolution detected or ex-

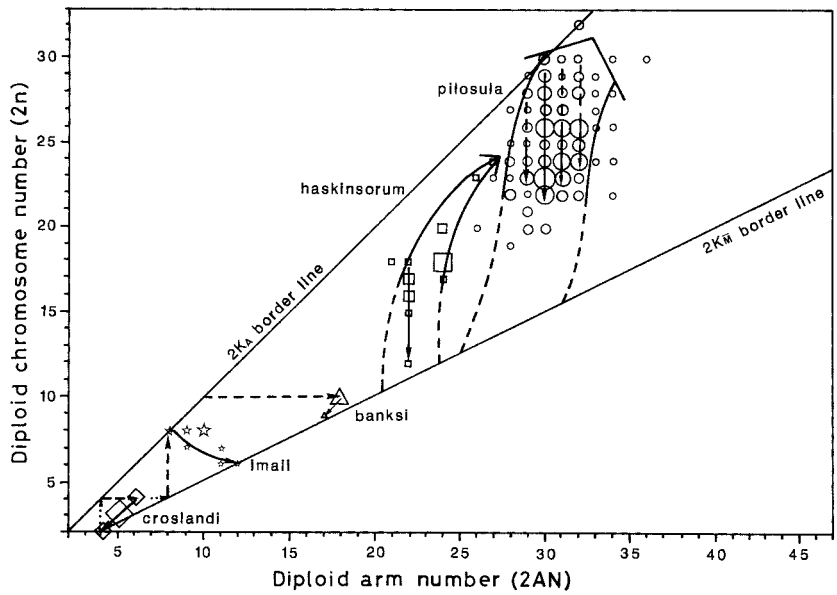

Fig. 20. Patterns of mass karyotype evolution in the *Myrmecia pilosula* species complex. Solid arrows indicate pathways actually detected, broken arrows or lines represent assumed pathways, based on karyotype analyses or karyotype distribution patterns, and dotted arrows are speculative pathways expected under the minimum interaction theory. See also Figs 12 and 19.

pected in the five species of the *pilosula* species complex are indicated by arrows superimposed on the karyograph, which is shown also in Fig. 12. Solid arrows indicate pathways actually detected; broken arrows or lines represent assumptions based on karyotype analyses or karyotype distribution patterns; and dotted arrows indicate hypothesized pathways expected under the minimum interaction theory.

Karyotype evolution in *M. croslandi* seems basically to have followed the compound pattern (1 + 4), but to have been modified by tandem fusion; $2\bar{M}$ – (c. fis) → 4A – (C^+) → $4A^M$ – (A$\bar{M}$-inv) → $2\bar{M} + 2A^M$ – (t. fus) → $2\bar{M}^{ci}$. This closed cycle of karyotype evolution is comparable to basic mode (c) discussed above, though tandem fusion (instead of centric fusion) has operated here to seal off the heterochromatic arm of the A^M chromosome.

The case of *M. imaii* could provide an example of compound pattern (1 + 5) (compare Figs 19d and 20), where the most probable pathway is $4\bar{M}$ – (c. fis) → 8A – (A$\bar{M}$-inv + c. fus) → $6\bar{M}$. The karyotype $2K = 4\bar{M}$ could be derived from 2K = 4A or ($2\bar{M} + 2A^M$) of *M. croslandi* by A$\bar{M}$-inversion, though direct evidence of this possibility has been lost in subsequent evolution.

M. banksi is karyotypically relatively conservative, and the karyotype $2K = 6\bar{M} + 2\bar{M}^c + 2A$ is quite different from the others involved in this account. If the four pairs of metacentrics were derived from acrocentrics by three independent A$\bar{M}$-inversions, the ancestral karyotype could be traced as 2K = 10A (i.e., basic pattern (4) in Fig. 19b). Under the minimum interaction theory the *banksi* karyotype would be expected to be highly stable because the amount of constitutive heterochromatin is very small and chromosomal interactions seem to be minimized (Fig. 15c).

The karyotypes of *croslandi*, *imaii*, and *banksi* seem to have evolved following an upwardly zigzag course between the two border lines of the karyograph, and would thus fall under compound patterns (1 + 4) or (1 + 5). The karyotype distributions of *M. pilosula* s. lat. and *M. haskinsorum* are, by contrast, quite different. They involve vertical dispersion, or, more precisely, the compound pattern (1 + 6) in *M. pilosula* s. lat. (Figs 12, 13, and 19e) and (1 + 8) in *M. haskinsorum* (Figs 12 and 19f). The origin of these karyotypes could be traced back to the metacentric karyotypes $2K = 10\bar{M} \sim 14\bar{M}$, but it is difficult to discern any direct karyological homology between these two species and those of the *pilosula* species complex with low numbers of chromosomes. The basic patterns (2), (3), (7), and (8) (Figs 19a and b) have not been identified in our studies of the *pilosula* species complex.

The arguments outlined above suggest strongly that evolutionary rates of chromosome rearrangement in the *M. pilosula* species complex have not been constant, but have fluctuated markedly. The same phenomenon was observed in mammalian karyotype evolution by Imai and Crozier (1980) and Imai, Maruyama and Crozier (1983), and in bees and wasps by Hoshiba and Imai (1993). A

detailed theoretical analysis of karyotype evolution using Monte Carlo simulation experiments will be published separately.

B. Mutability and stability of ant chromosomes

The ants (Formicidae) are taxonomically a mere family of the order Hymenoptera in class Insecta - yet they are cytologically highly diverse. As mentioned in the introduction, their known chromosome numbers range from $2n = 2$ to $2n = 94$, representing a span comparable to that of the whole class Mammalia, which has $2n = 6$ to $2n = 92$ (Matthey, 1973). Comparable ranges are known even at the levels of genera or species groups among ants. *Myrmecia*, for example, covers $2n = 2$ to $2n = 84$ (Imai, Crozier and Taylor, 1977; Imai et al., 1988a), and our present subject, the *Myrmecia pilosula* species complex, ranges from $2n = 2$ to $2n = 32$.

Mutability and stability of chromosomes may be considered two of the major factors responsible for the generation of such diversity. We now reconsider them in both the traditional context and that of the minimum interaction theory.

Mutability and stability of chromosomes in the traditional context: In traditional cytogenetics, two-break rearrangements have been adopted as standard among chromosomal mutations, and stability to selection has been considered an important factor in chromosome evolution (White, 1963, 1973).

Reciprocal translocation (Tr), inversion (In), and centric fusion (Fu) are the available rearrangements in this random-breakage-and-reunion model. Their theoretically expected relative frequencies are $Tr = 0.9467 - 0.9477$, $In = 0.0521 - 0.0527$, and $Fu = 0.0002 - 0.0006$ in humans and mice (Imai et al., 1988b). Thus, reciprocal translocation is the most common of the three, and centric fusion is negligibly rare.

Concerning the stability of these rearrangements, classical cytogeneticists have posited that only those rearrangements which are selectively neutral, or nearly so, can contribute to chromosome evolution. Reciprocal translocation is by this means deleterious, because more than 50% of gametes in heterozygotes become unbalanced due to nondisjunction. On the other hand, centric fusion was held to be selectively neutral, and for this reason to be one of the major rearrangements in chromosome evolution.

There are, however, data suggesting that centric fusion is not always selectively neutral. For example, in male European feral mice the incidence of nondisjunction in heterozygotes with a single centric fusion has been reported as 4-28% (Gropp et al., 1982), and the value increased to 100% in those individuals with multiple centric fusions (for example a ring of 16 or 18 chromosomes). It is important to understand that selective disadvantages as low as 4% are known from population genetics to be very effective in determining gene frequencies, except in very small populations.

According to the neutral theory (Kimura, 1983), even a rearrangement which is deleterious can be fixed by random drift in a small population where mutation rate is more important than stability to selection. Note that since centric fusion is selectively neutral in homozygotes, once it is fixed it is stable. Therefore, the fate of centric fusion in a small population is either that it will be eliminated at once, or that it will be fixed at once. In fact, the majority of centric fusions found in European feral mice have been fixed in each of the relevantly studied local populations (Capanna, 1982; Corti, Capanna and Estabrook, 1986).

Now, a simple question arises: why is it that only centric fusions were fixed in nature and not reciprocal translocations? The argument that reciprocal translocation is deleterious to selection is not persuasive. An alternative explanation provided by the minimum interaction theory is that reciprocal translocation seldom occurs in nature, and that once it has occurred it will be promptly eliminated by natural selection. If this is the case, another question arises: why does nature accept deleterious centric fusions as often as suggested by the evidence (Searle, 1993)?

Mutability and stability of chromosomes under the minimum interaction theory: It is important here to understand that all of the various chromosomal rearrangements-reciprocal translocation, centric fusion, centric fission, and A$\overline{\text{M}}$-inversion - are basically unstable in heterozygotes, but stable in homozygotes. The minimum interaction theory assumes that centric fission, centric fusion, and A$\overline{\text{M}}$-inversion are evolutionary adaptive because they reduce genetic risk. They are, however, double-edged rearrangements. Reciprocal translocation, on the other hand, has no comparable biological advantage. Moreover, it is potentially the major product if breakage and reunion occur at random (Imai et al., 1988b).

Two effective strategies may be prescribed to solve this problem, (1) reciprocal translocations occur abundantly in nature but are eliminated by selection, and (2) eukaryotes have mechanisms by which they avoid the occurrence of reciprocal translocations. The former implies the continual occurrence of a genetic load.

In the minimum interaction theory chromosomal rearrangements are assumed to take place under the hammock structure at pachytene, following the exchange model (Revell, 1974). In this situation the occurrence of chromosomal rearrangements is non-random. It is importantly characteristic that the frequency of reciprocal translocation is reduced drastically in those karyotypes with high chromosome numbers. Therefore, an increase in chromosome number by centric fission would be evolutionary adaptive. Centric fusion and A$\overline{\text{M}}$-inversion are also advantageous because they eliminate C-bands, which would increase markedly in frequency in telocentrics induced by centric fission, as discussed above.

Now, we will consider the possibility that our analysis of ant chromosome evolution presages a general model describing eukaryotic chromosome evolution.

Chromosome evolution in the haplo-diploid system: Sex determination in ants involves haplo-diploidy. Males develop by arrhenotoky from unfertilized eggs laid by the queens or unmated workers. They are genetically haploid (n) and lack meiosis. On the other hand, females - queens and the various worker castes - develop from fertilized eggs. They are genetically diploid (2n). The workers are generally reproductively subfertile and do not mate. With a few known exceptions, they do not have a role in the production of female offspring.

It is a peculiarity of ants that aneuploids (involving monosomy, trisomy, etc.), or unbalanced products of structural chromosomal rearrangements induced by nondisjunction, are often viable and, may even be fertile (Imai, Crozier and Taylor, 1977; Imai et al., 1985, 1988a). This phenomenon has been repeatedly observed in the research reported here, as indicated above. This suggests that selection pressure on alternative chromosomal rearrangements must be very low (perhaps essentially neutral) in these insects, with the result that a newly induced chromosomal rearrangement will survive for a relatively long time in ant populations.

As discussed above, population size is an important factor for stability of chromosomal rearrangements. In the case of our observations, local subject *Myrmecia pilosula*-group populations were separated by distances ranging from a few km to several tens of km, and colony numbers in each population are at most 1–20. Each colony comprised around 50 to 500 workers and one (or occasionally two) queen(s). Because the workers are reproductively neuter, genetically effective individuals thus number only one or two per colony and 2 to 40 per population. Therefore, the effective population size in taxa of the *M. pilosula*-group is very small. In other words, the effect of random drift could be high. Crozier (1981) suggested that a population size effect mediates the rate of ant karyotype evolution and the *Myrmecia pilosula* species complex fits this suggestion.

We observed chromosomes mainly from somatic cells taken from the brains of workers. Karyotypes were usually stable in the cells of each individual, except in the cases of the fission burst found in *M. pilosula* s. str., and C-band polymorphisms. Dissimilar karyotypes per colony numbered between 1 and 4 (mean 1.6). If each nest included 1 or occasionally 2 or more queens, and each queen had copulated with only 1 or occasionally 2 or more males, chromosomal heterogeneity in the *Myrmecia pilosula* species complex must largely reflect the genetic variability in the germ cells of queens.

No chromosomes of *banksi* origin were found in the putative later-generation hybrids between *pilosula* s. lat. and banksi (PB-hybrids). This suggests that, in the germ cells of the PBF_1 queens with $2K = (2\bar{M} + 2\bar{M}^c + 1A) + (1\bar{M}^{cc} + 8A + 3A^M + 1A^{Mc} + 1A^c)$, the parental haploid sets transmitted from *banksi* $(2\bar{M} + 2\bar{M}^c + 1A)$ and hybridizing elements of *pilosula* s. lat. $(1\bar{M}^{cc} + 8A + 3A^M + 1A^{Mc} + 1A^c)$ are completely separated except for genes exchanged by

crossing-over. These two haploid types could develop into males by arrhenotoky, and both would be viable and fertile. If such males backcross with *pilosula* s. lat. queens, the PBF_1 karyotype and PB-hybrid karyotypes, would again be expected. This breeding system is possible because of the presence of haplo-diploidy in ants. Note that, in higher organisms, a species with a karyotype such as PBF_1 would usually be sterile without the operation of a special mechanism found, for example, in the huntsman spider (Rowell, 1985) or the so-called Rabl orientation (Fussell, 1987).

Colonies in the *Myrmecia pilosula* species complex are often, perhaps usually, established by groups of queens (primary pleometrosis). We have observed, for example, as many as seven *pilosula* s. lat. founding queens nesting together under a single stone, and were able artificially to associate ten queens of *M. imaii* (HI91-1). This could provide an important mechanism by which the complicated chromosomal polymorphisms in *pilosula*-species-group populations are maintained. Supporting this, Craig and Crozier (1979) found low relatedness between worker nestmates in a population of this group. Further work is needed to examine geographical variation in these important biological characteristics, given that we now know that the group comprises a cluster of sibling species and not a single variable species.

Because F_1 hybrids in male-haploids such as ants can only be female, and that there is of course no male recombination, it may be that male-haploidy fosters the persistence of parental chromosome sets relatively unaltered, although the mechanism of this is unclear. In any case, the very high rate of chromosome evolution in this exceptional group of ants gives us an almost continuous pageant of karyotypes not observable in other animal groups. The picture we see in the *Myrmecia pilosula* species complex, we believe, enables us to integrate the fusion and fission views of karyotype evolution under the minimum interaction theory.

We thank Drs G. Browning, M. W. J. Crosland, G. Ettershank, M. Kubota, K. Ogata, and M. Wada, with S. Kuribayashi, Rev. B.B. Lowery and T. Terzis for their assistance with field work and the collection of specimens. Drs J. Oakeshott and A. Smigielski furnished valuable support and access to molecular-biological laboratory facilities in Canberra. Drs D. Bedo, B. Halliday, T. Matsumoto, K. Oishi, Y. Satta, and M. J. Whitten, and Y. Ching Crozier, Tokuko Imai, Renate Sadler, and Wendy Taylor provided invaluable support and encouragement. Large-scale field studies were supported by the Overseas Visitors Program of Division of Entomology, CSIRO, Australia (1985) and by Grants-in-Aid for Overseas Scientific Research from the Japanese Ministry of Education (1987, 1989). Ants for culture by HTI were sent to Japan with authority from the appropriate Australian Wildlife protection authorities. Taylor's recent researches on the taxonomy of *Myrmecia*, including species of the *pilosula* species complex, have been largely funded by The Australian Biological Resources Study (ABRS) Participatory Program. Crozier's research on evolutionary genetics, including that of the *M. pilosula* complex, has been supported by grants from the Australian Research Council, the Ian Potter Foundation, and La Trobe University.

REFERENCES

Blackburn, E. H. (1991). Structure and function of telomeres. *Nature* **350**, 569–573.

Browning, G. P. (1987). *Taxonomy of* Myrmecia *Fabricius (Hymenoptera: Formicidae).* PhD. Thesis. (Univ. of Adelaide).

Capanna, E. (1982). Robertsonian numerical variation in animal speciation: *Mus musculus*, an emblematic model. In: *Mechanisms of Speciation* (ed.: C. Barigozzi), pp. 155–177. Alan R. Liss, Inc., New York.

Clark, J. (1954). *The Formicidae of Australia.* Vol. 1. *Subfamily Myrmeciinae.* CSIRO, Melbourne.

Corti, M., Capanna, E. and Estabrook, G. F. (1986). Microevolutionary sequences in house mouse chromosomal speciation. *Syst. Zool.* **35**, 163–175.

Craig, R. and Crozier, R. H. (1979). Relatedness in the polygynous ant *Myrmecia pilosula. Evolution* **33**, 335–341.

Crosland, M. W. J. and Crozier, R. H. (1986). *Myrmecia pilosula*, an ant with only one pair of chromosomes. *Science* **231**, 1278.

Crosland, M. W. J., Crozier, R. H. and Imai H. T. (1988). Evidence for several sibling biological species centered on *Myrmecia pilosula* (F. SMITH) (Hymenoptera: Formicidae). *J. Aust. Entomol. Soc.* **27**, 13–14.

Fussel, C. P. (1987). The Rabl orientation: A prelude to synapsis. In: *Meiosis* (ed.: P. B. Moens), pp. 275–299. Academic Press, Orlando.

Crozier, R. H. (1981). Genetic aspects of ant evolution. In: *Essays in Evolution and Speciation in Honor of M. J. D. White* (eds: W.R. Atchley and D.C. Woodruff), pp. 356–370. Cambridge Univ Press, Cambridge, U.K.

Greider, C. W., Autexier, C., Avilion, A. A., Collins, K., Harrington, L. A., Mantell, L. L., Prowse, K. R., Smith, S. K., Allsopp, R. C., Counter, C. M., Vaziri, H., Bacchetti, S. and Harley, C. B. (1993). Telomeres and telomerase: biochemistry and regulation in senescence and immortalization. In: *The Chromosome* (eds: J. S. Heslop-Harrison and R. B. Flavell), pp. 115–125. Bios Scientific Publisher Limited, Oxford.

Gropp, A., Winking, H. and Redi, C. (1982). Consequences of Robertsonian heterozygosity: segregational impairment of fertility versus male-limited sterility. In: *Genetic Control of Gamete Production and Function* (eds: P. G. Crosignani and B. L. Rubin), pp. 115–151. Academic Press, London.

Hölldobler, B. and Wilson, E. O. (1990). *The Ants.* Belknap Press of Harvard University Press, Cambridge, Mass.

Hoshiba, H. and Imai, H. T. (1993). Chromosome evolution of bees and wasps (Apocrita, Hymenoptera) on the basis of C-banding pattern analyses. *Jpn. J. Ent.* **61**, 465–492.

Imai, H. T. (1975). Evidence for non-random localization of the centromere on mammalian chromosomes. *J. Theor. Biol.* **49**, 111–123.

Imai, H. T. (1976). Further evidence and biological significance for non-random localization of the centromere on mammalian chromosomes. *J. Theor. Biol.* **61**, 195–203.

Imai, H. T. (1978). On the origin of telocentric chromosomes in mammals. *J. Theor. Biol.* **78**, 619–637.

Imai, H. T. (1988). Centric fission in man and other mammals. In: *The Cytogenetics of Mammalian Autosomal Rearrangements* (ed.: A. Daniel), pp. 551–582. Alan R. Liss Inc., New York.

Imai, H. T. (1991). Mutability of constitutive heterochromatin (C-bands) during eukaryotic chromosomal evolution and their cytological meaning. *Jpn. J. Genet.* **66**, 635–661.

Imai, H. T. (1993). A theoretical approach to chromosome banding pattern analysis. *Jpn. J. Genet.* **68**, 97–118.

Imai, H. T. and Crozier, R. H. (1980). Quantitative analysis of directionality in mammalian karyotype evolution. *Am. Nat.* **116**, 537–569.

Imai, H. T. and Maruyama, T. (1978). Karyotype evolution by pericentric inversion as a stochastic process. *J. Theor. Biol.* **70**, 253–261.

Imai, H. T. and Taylor, R. W. (1989). Chromosomal polymorphisms involving telomere fusion, centromeric inactivation and centromere shift in the ant *Myrmecia (pilosula)* n = 1. *Chromosoma* **98**, 456–460.

Imai, H. T., Crozier, R. H. and Taylor, R. W. (1977). Karyotype evolution in Australian ants. *Chromosoma* **59**, 341–393.

Imai, H. T., Maruyama, T. and Crozier, R. H. (1983). Rates of mammalian karyotype evolution by the karyograph method. *Am. Nat.* **121**, 477–488.

Imai, H. T., Taylor, R. W., Crosland, M. W. J. and Crozier, R. H. (1988a). Modes of spontaneous chromosomal mutation and karyotype evolution in ants with reference to the minimum interaction hypothesis. *Jpn. J. Genet.* **63**, 159–185.

Imai, H. T., Maruyama, T., Gojobori, T., Inoue, Y. and Crozier, R. H. (1986). Theoretical bases for karyotype evolution. I. The minimum-interaction hypothesis. *Am. Nat.* **128**, 900–920.

Imai, H. T., Taylor, R. W., Kubota, M., Ogata, K. and Wada, M. Y. (1990). Notes on the remarkable karyology of the primitive ant *Nothomyrmecia macrops*, and of the related genus *Myrmecia* (HYMENOPTERA: FORMICIDAE). *Psyche* **97**, 133–140.

Imai, H. T., Takahata, N., Maruyama, T., Daniel, A., Honda, T., Matsuda, Y. and Moriwaki, K. (1988b). Theoretical bases for karyotype evolution. II. The fusion burst in man and mouse. *Jpn. J. Genet.* **63**, 313–342.

Imai, H. T., Baroni Urbani, C., Kubota, M., Sharma, G. P., Narasimhanna, M. N., Das, B. C., Sharma, A. K., Sharma, A, Deodikar, G. B., Vaidya, V. G. and Rajasekarasetty, M. R. (1985). Karyological survey of Indian ants. *Jpn. J. Genet.* **59**, 1–32.

Kimura, M. (1983). *The Neutral Theory of Molecular Evolution.* Cambridge University Press, Cambridge, UK.

Matthey, R. (1973). The chromosome formulae of eutherian mammals. In: *Cytotaxonomy and Vertebrate Evolution* (eds: A. B. Chiarelli and E. Capanna), pp. 531–616. Academic Press, London.

Ogata, K. (1991). Ants of the genus *Myrmecia* Fabricius: a review of the species groups and their phylogenetic relationships (Hymenoptera: Formicidae: Myrmeciinae). *Syst. Entomology* **16**, 353–381.

Ogata, K. and Taylor R. W. (1991). Ants of the genus *Myrmecia* Fabricius: a preliminary review and key to the named species (Hymenoptera: Formicidae: Myrmeciinae). *J. Nat. History* **25**, 1623–1673.

Revell, S. H. (1974). The breakage-and-reunion theory and the exchange theory for chromosomal aberrations induced by ionizing radiations: a short history. *Adv. Radiat. Biol.* **4**, 367–416.

Richards, E. J., Vongs, A., Walsh, M., Yang, J. and Chao, S. (1993). Substructure of telomere repeat arrays. In: *The Chromosome* (eds: J. S. Heslop-Harrison and R. B. Flavell), pp 115–125. Bios Scientific Publisher Limited, Oxford.

Rowell, D. M. (1985). Complex sex linked fusion heterozygosity in the Australian huntsman spider *Delena cancerides* (Araneae: Sparassidae). *Chromosoma* **93**, 169–176.

Searle, J. B. (1993). Chromosomal hybrid zones in eutherian mammals. In: *Hybrid Zones and the Evolutionary Process* (ed.: R. G. Harrison), pp. 309–353. Oxford University Press, New York.

Taylor, R. W. (1991). *Myrmecia croslandi* sp. n., a karyologically remarkable new Australian bulldog ant (Hymenoptera: Formicidae: Myrmeciinae). *J. Aust. Ent. Soc.* **30**, 288.

Todd, N. B. (1970). Karyotypic fissioning and canid phylogeny. *J. Theor. Biol.* **26**, 445–480.

Todd, N. B. (1975). Chromosomal mechanisms in the evolution of artiodactyls. *Paleobiology* **1**, 175–188.

White, M. J. D. (1963, 1973). *Animal Cytology and Evolution.* 2nd and 3rd ed. Cambridge University Press, London.

Willard, H. F. (1990). Centromeres of mammalian chromosomes. *Trends Genet.* **6**, 410–416.

Appendix: Karyological data of *Myrmecia pilosula* species complex

Species (Locality code in Fig.) Colony codes	2n (n)	2AN (AN)	No. ind. obs. ♀(♂)	Diploid karyotype 2K (Haploid karyotype K)	Remarks Chrom. polym. Fig. References
M. croslandi					
(5) HI87-148, 150, 151, 153, (7)157; HI89-030, 032	2	4	24	$2\overline{\overline{M}}^{ci}$	t. fus, Fig. 5a
(5) HI87-136, 148, 150, 153, (6)154; HI91-49	3	5	27	$1A^{M}+1\overline{\overline{M}}^{ci}+1\overline{\overline{M}}$	A$\overline{\overline{M}}$-inv Figs 5b, 15a
(5) HI87-136, (6)154	4	6	7	$2A^{M}+2\overline{\overline{M}}$	
(13) HI87-165	4	6	6	$2A^{c}+2\overline{\overline{M}}$	
(13) HI87-235	3	5	3	$1A^{c}+1\overline{\overline{M}}+1\overline{\overline{M}}^{ci}$	A$\overline{\overline{M}}$-inv
(13) HI87-235	4	6	8	$2A^{c}+1\overline{\overline{M}}+1\overline{\overline{M}}^{c}$	
(31) HI87-213; (5) HI89-030	3	5	11	$1A^{c}+1\overline{\overline{M}}+1\overline{\overline{M}}^{ci}$	c. sft
M. imaii					
(54) HI89-005, 006	8	8	2	$6A+2A^{M}$	
	(4)	(4)	(2)	$(3A+1A^{M})$	
(54) HI89-006	7	9	2	$3A+2A^{M}+1\overline{\overline{M}}+1\overline{\overline{M}}^{c}$	c. sft
(54) HI89-007	8	9	1	$1A+6A^{M}+1\overline{\overline{M}}$	A$\overline{\overline{M}}$-inv
(54) HI89-009	8	9	5	$4A+3A^{M}+1\overline{\overline{M}}$	A$\overline{\overline{M}}$-inv
(54) HI91-1	8	10	1	$1A+5A^{M}+2\overline{\overline{M}}^{t}$	Figs 5c, 15b
(54) HI91-3	8	10	3	$3A+3A^{M}+2\overline{\overline{M}}$	
(55) HI91-8	8	10	3	$6A^{M}+2\overline{\overline{M}}$	Fig. 5d
(55) HI91-8	7	11	1	$3A^{M}+4\overline{\overline{M}}^{c}$	c. fus (2), A$\overline{\overline{M}}$-inv, Fig. 5e
(56) HI91-5	8	8	1	$2A^{M}+6A$	
(56) HI91-5	6	11	2	$1A+5\overline{\overline{M}}^{c}$	c. fus (3), A$\overline{\overline{M}}$-inv (2), Fig. 5f
(56) HI91-5	6	12	1	$6\overline{\overline{M}}^{c}$	Fig. 5g
(56) HI91-5	(3)	(5)	(1)	$(1A+1\overline{\overline{M}}+1\overline{\overline{M}}^{c})$	
M. banksi					
(2) AAGR-13	10	18	3	$2A+6\overline{\overline{M}}+2\overline{\overline{M}}^{c}$	Imai et al. (1977)
(2) AAGT-11	10	18	1	$2A+6\overline{\overline{M}}+2\overline{\overline{M}}^{c}$	Imai et al. (1977)
(2) AAGT-11	9	17	1	$1A+6\overline{\overline{M}}+2\overline{\overline{M}}^{c}$	A$\overline{\overline{M}}$-inv, Comp. tr.

Appendix (continued-2)

Species (Locality code in Fig.) Colony codes	2n (n)	2AN (AN)	No. ind. obs. ♀(♂)	Diploid karyotype 2K (Haploid karyotype K)	Remarks Chrom. polym. Fig. References
					Imai et al. (1977)
(3) HI87-122-127	10	18	16	$2A+6\overline{M}+2\overline{M}^{c}$	
(10) HI87-158	10	18	4	$2A+6\overline{M}+2\overline{M}^{c}$	
(11) HI87-160	10	18	1	$2A+6\overline{M}+2\overline{M}^{c}$	
(4) HI89-034	10	18	3	$2A+6\overline{M}+2\overline{M}^{c}$	
(4) HI91-48	10	18	3	$2A+6\overline{M}+2\overline{M}^{c}$	Figs 5h, 15c
	(5)	(9)	(1)	$(1A+3\overline{M}+1\overline{M}^{c})$	
(9) HI85-213	10				
M. haskinsorum					
Corang River Bridge					
(5) HI87-152	23	26	4	$20A+2\overline{M}+1\overline{M}^{c}$	c. fis, Figs 6a, 15e
	24	27	3	$21A+2\overline{M}+1\overline{M}^{c}$	
Mt. Buffalo					
(27) HI87-224	20	24	4	$16A+2\overline{M}+2\overline{M}^{cc}$	c. fus, Fig. 6b
(27) HI87-225	(10)	(12)	(1)	$(8A+1\overline{M}+1\overline{M}^{cc})$	
Dead Horse Gap					
(22) HI87-233	18	22	1	$12A+2A^{M}+4\overline{M}^{c}$	Fig. 6e
	17	22	1	$10A+2A^{M}+3\overline{M}+2\overline{M}^{c}$	c. fis
	15	22	1	$6A+2A^{M}+3\overline{M}+4\overline{M}^{c}$	c. fus, Fig. 6f
	(8)	(11)	(1)	$(4A+1A^{M}+2\overline{M}+1\overline{M}^{c})$	
(22) HI87-234	12	22	5	$2A^{M}+6\overline{M}+4\overline{M}^{c}$	c. fus (4), Fig. 6h
(22) HI91-46	18	21	1	$13A+2A^{M}+1\overline{M}+2\overline{M}^{c}$	c. fis, c. fus
	15	23	1	$6A+1A^{M}+3\overline{M}+5\overline{M}^{c}$	A$\overline{M}$-inv (2), Fig. 6g
(22) HI91-47	17	22	1	$10A+2A^{M}+2\overline{M}+3\overline{M}^{c}$	
	(8)	(11)	(1)	$(3A+2A^{M}+3\overline{M}^{c})$	
(43) HI87-197-199	18	24	11	$12A+1\overline{M}+3\overline{M}^{c}+2\overline{M}^{cc}$	c. fis (1), c. fus (2), c. sft, Figs 6c, 15d
	17	24	3	$10A+5\overline{M}^{c}+2\overline{M}^{cc}$	c. fus (3), A$\overline{M}$-inv, Fig. 6d
	(9)	—	(1)	——	
(40) HI87-200	18	24	3	$10A+2A^{M}+2\overline{M}+4\overline{M}^{c}$	
	(9)	—	(1)	——	
(41) HI91-27	18	24	2	$12A+4\overline{M}+2\overline{M}^{c}$	
	(8)	(11)	(1)	$(5A+1\overline{M}^{c}+2\overline{M}^{cc})$	
	(9)	(12)	(2)	$(6A+2\overline{M}+1\overline{M}^{c})$	
(41) HI91-41	18	24	4	$12A+6\overline{M}^{c}$	

Appendix (continued-3)

Species (Locality code in Fig.) Colony codes	2n (n)	2AN (AN)	No. ind. obs. ♀(♂)	Diploid karyotype 2K (Haploid karyotype K)	Remarks Chrom. polym. Fig. References
M. pilosula s. str. MAINLAND					
(38) HI87-166-169	23	—	11		
	23	30		$1A^M+3A^c+12A+6\bar{M}+1\bar{M}^c$	c. fis (4), A$\bar{M}$-inv (2), Fig. 7e
	23	29		$12A+5A^c+6\bar{M}$	c. fis (3), A$\bar{M}$-inv
	23	31		$13A+2A^c+7\bar{M}+1\bar{M}^c$	c. fis (2), c. fus, A$\bar{M}$-inv
(37) HI87-170,171,173, 176	23	—	13		
	23	28		$13A+3A^M+2A^c+4\bar{M}+1\bar{M}^c$	c. fis
	23	29		$14A+1A^M+2A^c+5\bar{M}+1\bar{M}^c$	c. fis, c. fus, t. fis
	23	30		$15A+1A^c+6\bar{M}+1\bar{M}^c$	c. fis, c. fus
(35) HI87-177	28	—	3		
	28	31		$17A+4A^M+4A^c+2\bar{M}+1\bar{M}^c$	c. fis, c. fus, A$\bar{M}$-inv
	28	31		$21A+1A^M+3A^c+3\bar{M}$	
(35) HI87-178	26	30	2	$14A+4A^M+4A^c+3\bar{M}+1\bar{M}^c$	c. fus, A$\bar{M}$-inv
(36) HI87-181-185	22	28	1	$14A+2A^c+5\bar{M}+1\bar{M}^c$	c. fis, c. fus, A$\bar{M}$-inv
	23	31	4	$8A+4A^M+3A^c+6\bar{M}+2\bar{M}^c$	c. fis (2), c. fus, A$\bar{M}$-inv
	24	31	3	$11A+1A^M+5A^c+3\bar{M}+3\bar{M}^c+1\bar{M}^i$	c.fis(2),c.fus(3), t. fus, A$\bar{M}$-inv, Fig. 7f
	25	32	6	$11A+1A^M+6A^c+5\bar{M}+2\bar{M}^c$	c. fis (2), c. fus, t. fus, A$\bar{M}$-inv
	26	32	4	$12A+8A^c+1\bar{M}+4\bar{M}^c+1\bar{M}^i$	c. fis, c. fus, A$\bar{M}$-inv
	27	—	3	——	
(34) HI89-015,016	26	—	5	——	
	27	31	4	$16A+2A^M+5A^c+1\bar{M}+2\bar{M}^c+1\bar{M}^t$	c. fis, t. fis, c. fus (2), Fig. 7g
(33) HI89-020,021	26	31	1	$13A+8A^M+4\bar{M}+1\bar{M}^c$	A$\bar{M}$-inv
	29	30	2	$21A+7A^M+1\bar{M}$	c. fis
	30	30	2	$17A+13A^M$	
	(13)	(15)	(1)	$(11A+2\bar{M})$	
	(14)	(15)	(3)	$(12A+1A^M+1\bar{M})$	

Appendix (continued-4)

Species (Locality code in Fig.) Colony codes	2n (n)	2AN (AN)	No. ind. obs. ♀(♂)	Diploid karyotype 2K (Haploid karyotype K)	Remarks Chrom. polym. Fig. References
(32) HI87-214-218	27	31	4	$9A+14A^{M}+4\overline{M}$	Del.
	28	32	5	$9A+15A^{M}+4\overline{M}$	c. fis, $A\overline{M}$-inv
	29	30	1	$10A+18A^{M}+1\overline{M}$	c. fis
	29	32	1	$11A+15A^{M}+3\overline{M}$	$A\overline{M}$-inv (2)
	(14)	(16)	(3)	$(4A+8A^{M}+2\overline{M})$	
TASMANIA					
(49) HI87-186-188	24	—	1		
	24	31		$14A+3A^{M}+7\overline{M}$	c. fis (4), $A\overline{M}$-inv, Fig. 7c
	24	33		$9A+5A^{M}+1A^{c}+7\overline{M}+1\overline{M}^{c}+1\overline{M}^{cc}$	c. fis (3)
	24	31		$14A+3A^{M}+5\overline{M}+1\overline{M}^{c}+1\overline{M}^{cc}$	c. fis
	25	—	3		
	25	31		$16A+3A^{M}+6\overline{M}$	c. fis (4)
	25	31		$17A+2A^{M}+4\overline{M}+1\overline{M}^{c}+1\overline{M}^{cc}$	c. fis (3), $A\overline{M}$-inv
	26	—	7		
	26	32		$16A+3A^{M}+1A^{c}+4\overline{M}+1\overline{M}^{c}+1\overline{M}^{cc}$	c. fis (2)
	26	30		$17A+5A^{M}+2\overline{M}+1\overline{M}^{c}+1\overline{M}^{cc}$	
	26	31		$16A+3A^{M}+2A^{c}+4\overline{M}+1\overline{M}^{c}$	c. fis
	26	32		$17A+2A^{M}+1A^{c}+5\overline{M}+1\overline{M}^{cc}$	c. fis (2)
	26	32		$16A+2A^{M}+1A^{c}+5\overline{M}+1\overline{M}^{c}+1\overline{M}^{t}$	c. fis
	26	31		$17A+4A^{M}+3\overline{M}+2\overline{M}^{c}$	
	26	32		$13A+7A^{M}+4\overline{M}+2\overline{M}^{c}$	
	26	32		$17A+2A^{M}+1A^{c}+5\overline{M}+1\overline{M}^{c}$	
	26	32		$16A+4A^{M}+4\overline{M}+2\overline{M}^{cc}$	Fig. 7d
(46) HI87-195,196	21	29	2	$12A+1A^{M}+8\overline{M}$	c. fis (2)
	22	32	1	$11A+1A^{M}+10\overline{M}$	c. fis (2)
	24	30	2	$9A+8A^{M}+1A^{c}+4\overline{M}+2\overline{M}^{i}$	
	(11)	(15)	(2)	$(6A+1A^{M}+3\overline{M}+1\overline{M}^{c})$	
	(12)	(14)	(2)	$(9A+1A^{M}+2\overline{M})$	
	(12)	(15)	(2)	$(6A+3A^{M}+3\overline{M})$	

Appendix (continued-5)

Species (Locality code in Fig.) Colony codes	2n (n)	2AN (AN)	No. ind. obs. ♀(♂)	Diploid karyotype 2K (Haploid karyotype K)	Remarks Chrom. polym. Fig. References
(40) HI87-201,202; HI91-25,34	22	28	5	$13A+3A^{M}+6\overline{M}$	c. fis (3), c. fus
	23	29	8	$15A+1A^{M}+1A^{c}+5\overline{M}+1\overline{M}^{c}$	c. fis (4)
	24	32	3	$15A+1A^{c}+7\overline{M}+1\overline{M}^{c}$	c. fis (4), A$\overline{M}$-inv
(45) HI87-205,206	22	30	3	$8A+6A^{M}+8\overline{M}$	c. fus
	23	30	4	$11A+5A^{M}+7\overline{M}$	
	24	—	2	——	
(44) HI87-207,208	22		5		
	22	31		$11A+2A^{M}+9\overline{M}$	c. fis (3)
	22	30		$12A+1A^{M}+1A^{c}+8\overline{M}$	c. fis (4)
	23	30	1	$12A+4A^{M}+7\overline{M}$	c. fis
	24	31	2	$14A+3A^{M}+7\overline{M}$	c. fis
(44) HI87-209	22	—	1	——	
	23	30	1	$12A+4A^{M}+7\overline{M}$	c. fis
	(12)	(16)	2	$(4A+4A^{M}+3\overline{M}+1\overline{M}^{t})$	
(44) HI87-210	22		2	——	
	23	32	1	$10A+4A^{M}+8\overline{M}+1\overline{M}^{c}$	c. fis (3)
	(12)	(16)	(2)	$(3A+4A^{M}+1A^{c}+3\overline{M}+1\overline{M}^{t})$	
(44) HI91-35	(11)	(15)	(1)	$(4A+2A^{M}+1A^{c}+4\overline{M})$	
	(12)	(15)	(2)	$(4A+4A^{M}+1A^{c}+3\overline{M})$	
	(13)	(15)	(2)	$(5A+5A^{M}+1A^{c}+2\overline{M})$	
(44) HI91-36	23	30	2	$12A+4A^{M}+5\overline{M}+1\overline{M}^{t}+1\overline{M}^{c}$	c. fis (3), A$\overline{M}$-inv (2)
	24	—	2	——	
(47) HI91-18	(11)	(16)	(1)	$(2A+3A^{M}+1A^{c}+5\overline{M})$	
(48) HI91-19,20	22	31	2	$9A+2A^{M}+2A^{c}+8\overline{M}+1\overline{M}^{t}$	
	23	30	2	$10A+6A^{M}+7\overline{M}$	c. fis
	23	30	1	$13A+3A^{M}+6\overline{M}+1\overline{M}^{t}$	c. fis (2)
	26	30	1	$13A+9A^{M}+4\overline{M}$	c. fis (2)
	(11)	(15)	(1)	$(6A+1A^{M}+4\overline{M})$	
	(12)	(16)	(2)	$(5A+3A^{M}+4\overline{M})$	
(42) HI91-21,22	22		1	——	
	23	30	3	$13A+2A^{M}+1A^{c}+7\overline{M}$	c. fis
	24	32	1	$15A+1A^{M}+8\overline{M}$	c. fis (2)
	(12)	(17)	(2)	$(5A+2A^{c}+4\overline{M}+1\overline{M}^{t})$	
(53) HI91-29	(12)	(16)	(3)	$(8A+2\overline{M}+2\overline{M}^{c})$	

Appendix (continued-6)

Species (Locality code in Fig.) Colony codes	2n (n)	2AN (AN)	No. ind. obs. ♀(♂)	Diploid karyotype 2K (Haploid karyotype K)	Remarks Chrom. polym. Fig. References
	(13)	(16)	(2)	(8A+1A^{M}+1A^{c}+1$\overline{M}$ +2$\overline{M}^{c}$)	
(39) HI91-39,40,42-45	26	33	3	15A+4A^{M}+5$\overline{M}$+2$\overline{M}^{c}$	c. fis (3), c. fus
	27	33	6	14A+6A^{M}+1A^{c}+5$\overline{M}$ +1$\overline{M}^{c}$	c. fis (3), c. fus (2)
	(13)	(17)	(2)	(8A+1A^{M}+3$\overline{M}$+1$\overline{M}^{c}$)	
	(14)	(17)	(1)	(10A+1A^{M}+3$\overline{M}$)	
Hybrids between *M. pilosula* s. lat. and *M. banksi* (PB-hybrids)					
PBF$_1$-1 (F$_1$ karyotype)					
(6) HI87-155;	19	24	6	(1A+3$\overline{M}$+1$\overline{M}^{c}$)	
(7) HI87-156				+(8A+3A^{M}+1A^{Mc}	
				+1A^{c}+1$\overline{M}^{cc}$)	
(13) HI87-237;	19	24	9	(1A+3$\overline{M}$+1$\overline{M}^{c}$)	
HI85-372				+(8A+4A^{M}+1A^{c}	
				+1$\overline{M}^{cc}$)	Fig. 8
(13) HI85-373	18	23	4	(1A+3$\overline{M}$+1$\overline{M}^{c}$)	
				+(10A+1A^{M}+1A^{c}	
				+1$\overline{M}^{cc}$)	
PBF$_1$-2 (F$_1$ karyotype)					
(21) HI87-161,162	15	23	10	(1A+3$\overline{M}$+1$\overline{M}^{c}$)	
				+(2A+4A^{c}+1$\overline{M}$+3$\overline{M}^{c}$)	
PB-1					
(1) HI87-111-121	18	30	3	5A+1A^{c}+4$\overline{M}$+8$\overline{M}^{c}$	
	19	28	6	9A+1A^{M}+2$\overline{M}$+6$\overline{M}^{c}$	c. fus (7), A$\overline{M}$-inv,
				+1$\overline{M}^{cc}$	Fig. 11i
	20	26	9	10A+3A^{M}+1A^{c}+5$\overline{M}^{c}$	c. fus (5), A$\overline{M}$-inv,
				+1$\overline{M}^{cc}$	Fig. 11g
	21	29	8	11A+1A^{M}+1A^{Mc}+1$\overline{M}$	
				+7$\overline{M}^{c}$	
	22	30	9	11A+1A^{M}+2A^{c}+2$\overline{M}$	
				+4$\overline{M}^{c}$+2$\overline{M}^{cc}$	
	23	32	3	8A+6A^{M}+4$\overline{M}$+5$\overline{M}^{c}$	
	24	—	1	——	
	25	30	4	6A+12A^{M}+1A^{Mc}+1A^{c}	c. fus (4), Figs 11d,
				+1$\overline{M}$+2$\overline{M}^{c}$+1$\overline{M}^{cc}$+1$\overline{M}^{ct}$	15h
(19) HI87-128-130	28	29	1	9A+15A^{M}+3A^{c}+1$\overline{M}$	A$\overline{M}$-inv, Fig. 11a
	29	31	12	9A+11A^{M}+7A^{c}+2$\overline{M}$	
(18) HI87-131,132,133	24	32	8	3A+12A^{M}+1A^{c}+5$\overline{M}^{c}$	c. fus
				+3$\overline{M}^{cc}$	

Appendix (continued-7)

Species (Locality code in Fig.) Colony codes	2n (n)	2AN (AN)	No. ind. obs. ♀(♂)	Diploid karyotype 2K (Haploid karyotype K)	Remarks Chrom. polym. Fig. References
	24	31	2	$6A+11A^M+1\overline{M}+2\overline{M}^c+1\overline{M}^{ct}+3\overline{M}^{cc}$	c. fus
(17) HI87-134,135	22	—	1	——	
	23	31	2	$4A+11A^M+1\overline{M}+3\overline{M}^c+3\overline{M}^{cc}+1\overline{M}^i$	c. fus, t. fus, A$\overline{M}$-inv
	24	31	7	$7A+8A^M+2A^c+1\overline{M}+4\overline{M}^c+2\overline{M}^{cc}$	c. fus (2)
(12) HI87-141-145	32	32	23	$8A+24A^M$	Figs 11c, 15g
(16) HI87-146,147	23	30	7	$4A+12A^M+2\overline{M}^c+5\overline{M}^{cc}$	c. fus (4)
	24	29	2	$8A+11A^M+1\overline{M}+1\overline{M}^c+3\overline{M}^{cc}$	c. fus (4), t. fus, Fig. 11f
(31) HI87-211,212	27	28	2	$23A+3A^M+1\overline{M}$	c. fis
	28	33	1	$15A+8A^M+5\overline{M}$	A$\overline{M}$-inv
	29	33	8	$17A+8A^M+4\overline{M}$	c. fis, t. fus
(30) HI87-219	30	31	3	$8A+21A^M+1\overline{M}$	A$\overline{M}$-inv, Fig. 11b
(29) HI87-220,221	30	30	3	$9A+21A^M$	
	(15)	(16)	(3)	$(4A+10A^M+1\overline{M})$	A$\overline{M}$-inv
	(15)	(18)	(1)	$(4A+8A^M+3\overline{M})$	A$\overline{M}$-inv (2)
(28) HI87-222,223	22	—	1	——	
	23	30	4	$5A+10A^M+1AM^c+2\overline{M}+5\overline{M}^{cc}$	c. fus
	24	—	1	——	
	30	31	1	$9A+20A^M+1\overline{M}$	A$\overline{M}$-inv
(27) HI87-226	(15)	(17)	(3)	$(4A+9A^M+2\overline{M})$	
(24) HI87-227-229	22	29	5	$6A+9A^M+2\overline{M}+5\overline{M}^c$	c. fus
	23	29	3	$5A+12A^M+1\overline{M}+5\overline{M}^c$	c. fus
(23) HI87-231,232	23	27	3	$2A+17A^M+1\overline{M}+3\overline{M}^c$	
	23	29	2	$3A+14A^M+3\overline{M}^c+3\overline{M}^{cc}$	
(26) HI89-022-025	28	29	8	$21A+4A^M+2A^c+1\overline{M}$	A$\overline{M}$-inv
	29	29	8	$12A+10A^M+7A^c$	
(25) HI89-026-028	26	—	1	——	
	28	30	10	$12A+11A^M+3A^c+2\overline{M}$	A$\overline{M}$-inv (2)
(15) HI89-033 PB-2	32	32	5	$10A+22A^M$	
(5) HI87-137-140	22	—	1	——	
	23	—	5	——	
	24	—	8	——	
	25	32	4	$8A+4A^M+6A^c+2\overline{M}+3\overline{M}^c+2\overline{M}^{cc}$	c. fis, c. fus (4), A$\overline{M}$-inv (2), Fig. 11e

Appendix (continued-8)

Species (Locality code in Fig.) Colony codes	2n (n)	2AN (AN)	No. ind. obs. ♀(♂)	Diploid karyotype 2K (Haploid karyotype K)	Remarks Chrom. polym. Fig. References
	26	31	2	$13A+6A^{M}+2A^{c}+1\overline{M}+3\overline{M}^{c}+1\overline{M}^{cc}$	
(20) HI87-163,164	20	29	6	$4A+1A^{M}+6A^{c}+1\overline{M}+7\overline{M}^{c}+1\overline{M}^{cc}$	c. fus (6), A$\overline{M}$-inv, Fig. 11h
	(10)	(15)	(1)	$(3A+2A^{c}+1\overline{M}+3\overline{M}^{c}+1\overline{M}^{cc})$	
	26	32	4	$1A+15A^{M}+4A^{c}+2\overline{M}+3\overline{M}^{c}+1\overline{M}^{cc}$	
P/PB-1 Mix					
(52) HI87-191,192	25	31	2	$13A+6A^{c}+4\overline{M}+1\overline{M}^{c}+1\overline{M}^{ct}$	c. fus, t. fus, A$\overline{M}$-inv
	26	29	6	$18A+5A^{c}+3\overline{M}$	
	27	30	1	$18A+6A^{c}+3\overline{M}$	
	28	30	1	$18A+2A^{M}+6A^{c}+2\overline{M}$	
(46) HI87-193	22	31	1	$10A+3A^{M}+9\overline{M}$	c. fis
	23	30	1	$14A+2A^{M}+7\overline{M}$	c. fis, Fig. 7a
	(11)	(17)	(1)	$(4A+1A^{M}+6\overline{M})$	
	(13)	(17)	(1)	$(8A+1A^{M}+4\overline{M})$	
(50) HI87-203,204	25	28	1	$13A+3A^{M}+4A^{c}+2A^{Mc}+3\overline{M}$	c. fis (2), t. fis, Del.
	26	29	9	$15A+4A^{M}+4A^{c}+3\overline{M}$	c. fis (3), t. fis
(42) HI91-23	23	30	2	$13A+2A^{M}+1A^{c}+7\overline{M}$	c. fis (2)
	24	29	1	$12A+5A^{M}+2A^{c}+5\overline{M}$	c. fis (3), A$\overline{M}$-inv (2)
(40) HI91-26,28	22	30	4	$8A+3A^{M}+2A^{c}+9\overline{M}$	c. fis
	23	31	1	$12A+3A^{M}+8\overline{M}$	c. fis (2)
	(10)	(15)	(1)	$(4A+1A^{M}+4\overline{M}+1\overline{M}^{c})$	
	(11)	(15)	(1)	$(5A+1A^{M}+1A^{c}+4\overline{M})$	
	(12)	(14)	(2)	$(7A+1A^{M}+2A^{c}+1\overline{M}+1\overline{M}^{c})$	
	(12)	(15)	(2)	$(6A+1A^{M}+2A^{c}+2\overline{M}+1\overline{M}^{c})$	
P/PB-2 Mix					
(46) HI87-194	23	31	4	$9A+6A^{M}+6\overline{M}+2\overline{M}^{c}$	c. fis, A$\overline{M}$-inv, Figs 7b, 15f
	24	—	1	——	
(40) HI91-33	23	31	3	$14A+1A^{M}+6\overline{M}+2\overline{M}^{c}$	A$\overline{M}$-inv
(51) HI87-189,190	27	29	1	$21A+3A^{M}+1A^{c}+1\overline{M}+1\overline{M}^{t}$	c. fis, t. fis
	28	30	9	$23A+1A^{M}+2A^{c}+2\overline{M}$	c. fis, t. fis, A$\overline{M}$-inv

Appendix (continued-9)

Species (Locality code in Fig.) Colony codes	2n (n)	2AN (AN)	No. ind. obs. ♀(♂)	Diploid karyotype 2K (Haploid karyotype K)	Remarks Chrom. polym. Fig. References
(52) HI87-191; HI91-16,17	25	—	1		
	26	30	4	$16A+5A^{M}+1A^{c}+4\bar{M}$	t. fis
	27	30	4	$19A+4A^{M}+1A^{c}+3\bar{M}$	c. fis, t. fis